

*Shifting baseline in macroecology?
Unraveling the influence of human impact
on mammalian body mass*

Article

Accepted Version

Santini, L., González-Suárez, M. ORCID:
<https://orcid.org/0000-0001-5069-8900>, Rondinini, C. and Di
Marco, M. (2017) Shifting baseline in macroecology?
Unraveling the influence of human impact on mammalian body
mass. *Diversity and Distributions*, 23 (6). pp. 640-649. ISSN
1472-4642 doi: <https://doi.org/10.1111/ddi.12555> Available at
<https://centaur.reading.ac.uk/69201/>

It is advisable to refer to the publisher's version if you intend to cite from the
work. See [Guidance on citing](#).

To link to this article DOI: <http://dx.doi.org/10.1111/ddi.12555>

Publisher: Wiley

All outputs in CentAUR are protected by Intellectual Property Rights law,
including copyright law. Copyright and IPR is retained by the creators or other
copyright holders. Terms and conditions for use of this material are defined in
the [End User Agreement](#).

www.reading.ac.uk/centaur

CentAUR

Central Archive at the University of Reading

Reading's research outputs online

1 **Article type:** Original article

2 **Title:** Shifting baseline in macroecology? Unraveling the influence of human impact
3 on mammalian body mass

4 **Running head:** Human impact on mammalian body mass patterns
5

6 Luca Santini^{1,2*}, Manuela González-Suárez^{3,4}, Carlo Rondinini², Moreno Di Marco^{5,6}

7

8 ¹ Department of Environmental Science, Radboud University, P.O. Box 9010, NL-
9 6500 GL, Nijmegen, The Netherlands

10 ² Global Mammal Assessment program, Department of Biology and Biotechnologies,
11 Sapienza Università di Roma, Viale dell'Università 32, 00185 Rome, Italy

12 ³ Department of Conservation Biology, Estación Biológica de Doñana - CSIC, 41092
13 Seville, Spain.

14 ⁴ Ecology and Evolutionary Biology, School of Biological Sciences, University of
15 Reading, Whiteknights, Reading, Berkshire, RG6 6AS, UK

16 ⁵ ARC Centre of Excellence for Environmental Decision, Centre for Biodiversity and
17 Conservation Science, The University of Queensland, St Lucia, QLD 4072 (Brisbane,
18 Australia).

19 ⁶ School of Earth and Environmental Sciences, The University of Queensland, St
20 Lucia, QLD 4072 (Brisbane, Australia).

21

22 **Corresponding author:** Luca Santini, luca.santini.eco@gmail.com

23

24 **Abstract**

25 **Aim** Human activities have led to hundreds of species extinctions and have narrowed
26 the distribution of many of the remaining species. These changes influence our
27 understanding of global macroecological patterns, but their effects have been rarely
28 explored. One of these patterns, the Bergmann's rule, has been largely investigated in
29 macroecology, but often under the assumption that observed patterns reflect "natural"
30 processes. We assessed the extent to which humans have re-shaped the observable
31 patterns of body mass distribution in terrestrial mammals, and how this has altered the
32 macroecological baseline.

33 **Location** Global

34 **Methods** Using a comprehensive set of ecological, climatic, and anthropogenic
35 variables we tested several alternative hypotheses to explain the body mass pattern
36 observed in terrestrial mammals assemblages at a 1-degree resolution. We then
37 explored how model predictions and the Bergmann's latitudinal pattern are affected
38 by the inclusion of human impact variables, and identified areas where predicted body
39 mass differs from the expected due to human impact.

40 **Results** Our model suggests that median and maximum body mass predicted in grid
41 cells would be higher, and skewness in local mass distributions reduced, if human
42 impacts were minimal, especially in areas that are highly accessible to humans and
43 where natural land cover has been converted for human activities.

44 **Main conclusions** Our study provides evidence of the pervasive effects of
45 anthropogenic impact on nature, and shows human-induced distortion of global
46 macroecological patterns. This extends the notion of "shifting baseline", suggesting
47 that when the first macroecological investigations started, our understanding of global
48 geographic patterns was based on a situation which was already compromised. While

49 in the short term human impact is causing species decline and extinction, in the long
50 term it is causing a broad re-shaping of animal communities with yet unpredicted
51 ecological implications.

52

53 **Keywords:** Accessibility, Bergmann's rule, Defaunation, Extinction, Human impact,

54 Land use change, Terrestrial mammals, Vulnerability

55

56 **1. Introduction**

57 The current human impact on nature is pervasive, and land-use change has
58 considerably reshaped the Earth's surface and disrupted natural dynamics (Newbold
59 et al., 2016). Hundreds of vertebrate species have become extinct in the last centuries,
60 and many of the remaining species have shown declines in abundance and
61 contractions in distribution (Dirzo et al., 2014). The extent of these changes has led to
62 an alteration of natural macroecological patterns (Murray & Dickman, 2000; Diniz-
63 Filho et al., 2009; Di Marco & Santini, 2015a; Faurby & Svenning, 2015; Torres-
64 Romero & Olalla-Tárraga, 2015), to the point that current patterns may have become
65 a poor reflection of the original biogeographical drivers (Di Marco & Santini, 2015a;
66 but see Olalla-Tárraga et al., 2015; Di Marco & Santini, 2015b).

67 Since Bergmann's prediction that animal body mass increased with latitude
68 (Bergmann, 1847), the intra- and interspecific spatial distribution of body mass has
69 been one of the most investigated global macroecological patterns (Blackburn et al.,
70 1999; Meiri, 2011). However, after more than 160 years, the so-called Bergmann's
71 rule is still under debate (Blackburn et al., 1999; Meiri, 2011) with a number of
72 alternative explanations proposed. The original explanation by Bergmann has taken
73 the name of "heat conservation hypothesis" and predicts that organisms in colder
74 areas tend to be larger because the reduction in their surface/volume ratio that results
75 from increased size limits heat dissipation (Bergmann, 1847). Size may also affect the
76 evaporative cooling rate in moist and warm climate, favouring small-bodied species
77 (the "heat dissipation hypothesis"; Brown & Lee, 1969; James, 1970; Speakman &
78 Król, 2010). A larger body mass can reduce the risk of starvation as proposed by the
79 "starvation resistance hypothesis", allowing a species to cope with the seasonal
80 shortage of resources that occur in higher latitudes (Calder, 1984; Lindstedt & Boyce,

81 1985; Dunbrack & Ramsay, 1993). Larger species also disperse longer distances,
82 which could have influenced their ability to re-colonize high latitudes after the
83 Pleistocene ice-sheet retreat, as proposed in the “dispersal hypothesis” (Blackburn &
84 Hawkins, 2004). Finally, the “resource-rule” suggests that the pattern may arise from
85 the latitudinal pattern of resources availability reflecting gradients of climate and
86 biological competition (McNab, 2010). No hypothesis alone is able to explain the
87 observed patterns for all taxa, and several non-exclusive explanations have found
88 empirical support (Rodríguez et al., 2006; Rodríguez et al., 2008; Diniz-Filho et al.,
89 2009; Olson et al., 2009). Interestingly, all proposed mechanisms assume that
90 observable patterns are determined by “natural” environmental conditions, largely
91 disregarding past and present human impacts.

92 Investigation of the distribution of mammalian body mass and how humans
93 have changed observable patterns is of direct relevance for conservation assessments.
94 Species vulnerability to extinction is generally positively correlated with body mass.
95 Large species are at much higher risk than small ones (Purvis et al., 2000; Cardillo et
96 al., 2005; Di Marco et al., 2014a) and have a higher probability of facing an increase
97 in risk over time (Di Marco et al., 2015). This is because large species tend to live at
98 low densities (Damuth, 1981) and have slow rates of population growth as compared
99 to small species (Fenchel, 1974; Johnson, 2002). In addition, large-bodied mammals
100 have been largely persecuted by humans for meat (Milner-Gulland & Bennet, 2003;
101 Corlett, 2007), to reduce conflicts with human activities (Woodroffe, 2000), or for
102 trophy hunting (Allendorf & Hard, 2009). Scattered evidence suggests that the spatial
103 patterns in body mass that we observe today have been influenced by past human
104 impact, including human-induced megafauna extinctions in the Pleistocene (Smith &
105 Lyons, 2011; Morales-Castilla et al., 2012), and large fauna extinctions from

106 agricultural development in historical times (Fritz et al., 2009). More recent
107 extinctions, as well as contractions of species' geographic ranges (Diniz-Filho et al.,
108 2009; Di Marco & Santini, 2015a; Faurby & Svenning, 2015) may have also played a
109 central role in re-shaping global species assemblages (Ripple & Van Valkenburgh,
110 2010). Indeed, there are only a few areas worldwide left where the megafauna can be
111 considered intact (Morrison et al., 2007; Faurby & Svenning, 2015). It has also been
112 argued that the skewness of the distribution of mammal body mass in the Holocene
113 has been exacerbated due to the extinction large species in the Pleistocene (Lyons et
114 al., 2004; Smith & Lyons, 2011). Simulations have also suggested that the non-
115 random extinction of large-bodied species has likely contributed to the observed
116 skewness in body mass distribution (Maurer et al., 1992). Characterizing human
117 impacts on body size distributions can help us identifying altered mammalian
118 assemblages and more pristine and potentially sensitive communities.

119 Here we investigate how ecological, climatic, and anthropogenic variables
120 predict the current distribution of body mass in mammal species assemblages using a
121 1-degree grid covering the world's land surface. We then predict how body mass
122 values would change if the effects of human impact were minimal and whether the
123 relationship between latitude and body mass (Bergmann's rule) has been distorted by
124 human impact as has previously been argued (Faurby & Araújo, 2016). We
125 hypothesize that mammal species assemblages have overall reduced body size in
126 proportion to the intensity and duration of human impacts. We also hypothesize that
127 the skewness in body mass distribution has been increased by the loss of large
128 species. Furthermore, because human impacts are not homogenously distributed
129 across the planet, we expect a weaker relationship between latitude and body mass in
130 the Northern hemisphere, where impacts are predominant.

131

132 **2. Methods**

133 2.1. Spatial grid of body mass distribution

134 We analysed data for 5,242 terrestrial mammal species for which distribution and
135 body mass information were available (~98% of all terrestrial mammals). We used the
136 geographic range polygons published by the Red List of the International Union for
137 Conservation of Nature to represent species distributions (IUCN, 2015), and obtained
138 body mass data from Pacifici et al. (2013) which is largely based on the PanTHERIA
139 dataset (Jones et al., 2009). We analysed the geographical pattern of body mass at the
140 assemblage level (Olalla-Tárraga et al., 2010), and used a 1-degree resolution grid (in
141 lat-long) covering the world's lands whereby species were assigned to cells which
142 were entirely or partly overlapping with their ranges. Assemblage level approaches
143 are ideal to investigate the geographical pattern of the Bergmann' rule because they
144 allow to directly assess the underlying environmental structure. With alternative
145 cross-species approaches this structure would be severely limited because
146 environmental gradients are reduced to a single point in the geographical space
147 (Olalla-Tárraga et al., 2010). For each grid cell, we then calculated the median,
148 maximum and skewness of untransformed body mass values (Fig. 1; Meiri &
149 Thomas, 2007). We excluded from analyses cells with ≤ 5 species. The maximum was
150 expressed as the 90th percentile of the statistical distribution of body mass values in
151 order to avoid capturing outliers (Blackburn & Hawkins, 2004) , and it was only
152 calculated for cells with >10 species.

153

154 2.2. Environmental and human impact variables

155 We considered 12 potential environmental predictors of species body mass following
156 previous macroecological research on body mass distribution in endotherms. We
157 represented climatic conditions considering: mean annual temperature, mean
158 temperature of the coldest quarter, mean temperature of the warmest quarter, mean
159 annual precipitation, mean precipitation of the driest quarter, mean precipitation of the
160 wettest quarter, and actual evapotranspiration (AET). Temperature is directly linked
161 with the heat conservation hypothesis, whereas precipitation and AET are linked to
162 the heat dissipation hypothesis (Blackburn & Hawkins, 2004; Rodríguez et al., 2006;
163 Rodríguez et al., 2008; Diniz-Filho et al., 2009; Olson et al., 2009). Temperature and
164 precipitation variables were downloaded from WorldClim (Hijmans et al., 2005) for
165 the period 1950-2000. AET and PET were downloaded from
166 <http://www.grid.unep.ch/data/summary.php?dataid=GNV183> for the period 1920-
167 1980. Additionally as a measure of mesoscale climatic variation and environmental
168 heterogeneity within cells (Blackburn & Hawkins, 2004; Rodríguez et al., 2006;
169 Rodríguez et al., 2008; Diniz-Filho et al., 2009; Olson et al., 2009) we used the range
170 in elevation calculated from the global relief model ETOPO1 (Amante & Eakins,
171 2009). We represented primary productivity using the Normalized Difference of
172 Vegetation Index (NDVI;
173 http://neo.sci.gsfc.nasa.gov/view.php?datasetId=MOD13A2_M_NDVI). We used
174 monthly estimates from 2000 to 2012 to calculate annual mean productivity and the
175 coefficient of variation in NDVI within year as a proxy of seasonality in primary
176 productivity (Blackburn & Hawkins, 2004; Rodríguez et al., 2006; Rodríguez et al.,
177 2008; Diniz-Filho et al., 2009; Olson et al., 2009). The periods represented by these
178 variables differ because data were not available for the same periods. To account for
179 historical processes that could influence body mass distribution we estimated "time

180 since last glacial retreat" following Rodríguez et al. (2006). Finally, body mass values
181 in an area might be influenced by species richness (Meiri & Thomas, 2007; Olson et
182 al., 2009), hence we controlled for this potential influence by including taxonomic
183 Order richness as a predictor. We used Order richness because it is more robust to
184 recent local extinctions than species richness, and thus more adequate when making
185 predictions that assumed no human impacts (see below). We acknowledge that this
186 approach has potential limitations for smaller orders, characterised by few large-
187 bodied species (e.g. Proboscidea, Perissodactyla), yet, for most groups that include
188 many of the largest mammals (e.g., Carnivora and Cetartiodactyla) it would be more
189 robust.

190 We additionally considered four variables representing levels of human impact
191 on natural environments: human population density (ind/ha) in the year 2000 (CIESIN
192 & CIAT, 2005); percentage of agricultural land calculated from Globcover satellite
193 images at year 2009 (IONIA, 2009); accessibility, expressed as travel time (hours)
194 from major cities (>50,000 people; Nelson, 2008); and history of land use, expressed
195 as time from first human use, spanning from 0 (never used) to 8000 (first used in 6000
196 bc), derived from the KK10 model of historical land use intensity (Ellis et al., 2013).
197 Following Ellis *et al.* (2013) we considered a cell as significantly used when the
198 percentage of land classified as human use was >20%.

199

200 2.3. Statistical analyses

201 To avoid potential collinearity issues (see Table S1 in Supporting Information) in
202 model fitting and to reduce model complexity, we performed a principal component
203 analysis (PCA). Prior to perform the PCA, mean annual precipitation, mean
204 precipitation of the wettest quarter, mean precipitation of the driest quarter, AET,

205 range in elevation, order richness and NDVI seasonality were log₁₀-transformed to
206 reduce distribution skewness, and all variables were standardized to a mean of zero
207 and a SD of one. To determine the number of components to retain we tested axes
208 significance based on the broken-stick criterion (Legendre & Legendre, 1998). We
209 selected the first two components that were significant and together explained 64.3%
210 of the variance (Table S2-S3).

211 We then fitted and compared alternative models to predict either the median or
212 maximum body mass values (log₁₀-transformed to meet model assumptions) in each
213 grid cell (Table 1). The null model included only the selected principal components
214 reflecting environmental characteristics. Additional models were built by adding
215 combinations of one or two human impact variables (Table 1). Some combinations of
216 impact variables were not tested because of high correlation among variables (Pearson
217 $r \geq 0.7$). All human impact variables were also log₁₀-transformed to meet linearity
218 assumptions in our models. Because large bodied species need large areas to form
219 viable populations, body mass is also constrained by island size. In order to account
220 for area constraints in body mass all models were also run including the factor
221 “islands” to allow the intercept to adjust at different values. Islands were defined as
222 all land masses smaller than an area threshold. We defined 4 thresholds: 25,000 km²
223 (102 cells), 100,000 km² (231 cells), 500,000 km² (386 cells), and 7,500,000 km² (724
224 cells; ~ all lands smaller than Australia).

225 Each model was first fitted using ordinary least square regression (OLS) and
226 we tested for spatial autocorrelation in the residuals using Moran Index. Because
227 models’ residuals were always significantly autocorrelated (Table S4), we used spatial
228 auto-regressive linear models (SAR) with a rook neighbourhood to compare proposed
229 models and estimate coefficients. We used the function “errorsarlm” from the package

230 “spdep” in R 3.0.3 (R Core Team, 2016). This spatial error model assumes that the
231 autoregressive process is found only in the error term, and it has been found to
232 perform better than OLS and other SAR models (Kissling & Carl, 2008). This
233 approach removed most of the spatial autocorrelation in the residuals (Fig. S1).

234 Models were compared using Bayesian Information Criterion (BIC) weights
235 (ω), indicating the relative weight of evidence of competitive models (Burnham &
236 Anderson, 2002). We used BIC rather than the more commonly used Akaike
237 Information Criterion (AIC) because it is more conservative in estimating differences
238 between competitive models when sample size is high ($n > 15,000$ in this study) and
239 tends to select for simpler, more parsimonious models (Raffalovich et al., 2008).
240 However, for comparison, we also report the results of model selection based on AIC
241 in supporting material (Table S7). Following Burnham and Anderson (2002) we
242 calculated predicted values based on a single model if clearly identified as best ($\omega >$
243 0.9) or using weighted estimates obtained by averaging predictions of all models
244 weighted by ω . We calculated the variance explained by the models as pseudo- R^2 , by
245 taking the square of the correlation coefficient between the fitted values and the
246 observed variable (R^2_{sp}), and the square of the correlation coefficient between the
247 predicted values using the coefficients only (not the spatial part) and the observed
248 variable (R^2_{nsp}). While the former indicate the variance explained by the fixed factor
249 and the spatial autocorrelation combined, the latter indicate the variance explained by
250 the fixed factors only. The model selection procedure described above was replicated
251 using skewness in body mass as the response variable. Mammalian body mass
252 distribution has been shown to be both phylogenetically and spatially autocorrelated
253 at a global scale (Villalobos et al., 2016). However, phylogenetic relatedness in
254 assemblage-level analyses is a substantially smaller problem than in cross-species

255 analyses, and the method proposed to control for both spatial and phylogenetic
256 autocorrelation in assemblage-level analyses (eigenvector regression) (Diniz-Filho et
257 al., 1998, 2009) has been criticized (Adams & Church, 2011; Freckleton et al., 2011).

258 Using the SAR models, we then predicted mean and maximum body mass per
259 grid under two scenarios of anthropogenic impact: observed impact and minimal
260 impact. The first scenario corresponded to the fitted values from the best model (or a
261 ω -weighted average prediction from all models if no single model was clearly
262 supported). For the second scenario, we simulated minimal human impacts by
263 assigning to each grid cell the lowest observed value of each human impact variable
264 in the model, while retaining the environmental variable values, and recalculating its
265 predicted mean and maximum body mass (as above by weighted average if no single
266 model was clearly supported). To estimate the expected loss in median and maximum
267 body mass, we then calculated the difference (delta) between the predictions under the
268 two scenarios of human impact.

269 To assess whether Bergmann's rule is affected by human impact, we explored
270 the relationship between latitude and predicted body mass for each scenario. To avoid
271 longitudinal autocorrelation in these analyses, we treated longitudinal bands as
272 random effects (1 degree of longitude) and then modelled these mass values as a
273 function of latitude allowing for separate intercept and slope estimates for each
274 scenario. We used the function "lme" from the package "nlme". Because the observed
275 relationship between latitude and body mass is non-linear with an inflection around
276 20°N, we actually fitted three linear regression models: above 20° of latitude in the
277 northern hemisphere, between 0° and 20°N, and southern hemisphere. All spatial
278 analyses were performed using the package "raster" (Hijmans et al., 2005) and
279 "maptools" (Lewin-Koh & Bivand, 2011) in R 3.0.3 (R Core Team, 2016).

280

281 2.4. Comparison with historical data

282 As a mean of cross-validation, we compared the results obtained with our approach
283 based only on contemporary data with calculated differences in current vs. historical
284 body mass distributions (Faurby & Araújo, 2016). We calculated historical mean and
285 maximum body mass per cell using the historical ranges available from Faurby &
286 Svenning (2015) following the same procedure described above for the current ranges
287 (Fig. S2). Because our approach is likely to only capture relatively recent
288 anthropogenic effects, we only retained species recognized by the IUCN in the
289 historical dataset, which correspond to those persisting at least until 1,500 AD. Body
290 mass estimates for extinct species were primarily obtained from Smith *et al.* (2003),
291 and supplemented with data from publications on specific species (MacPhee &
292 Grimaldi, 1996; Goodman et al., 2004; van Vuure, 2005; Faurby & Svenning, 2016).
293 For extinct species for which no estimate was available we used the mean body mass
294 from its congeners. We calculated the agreement between both estimates simplifying
295 the change in body mass between current and historical species distribution to a
296 binary response (predicted decrease in mass=1, no decrease or increase=0). This
297 simplification allows measuring the agreement of the two models in terms of areas
298 where large-bodied species have been lost, rather than an agreement in the exact
299 values that was not expected *a priori* given the differences in the methodologies and
300 in the group of species considered. To quantify the overall agreement we estimated
301 the Area Under the Curve (AUC) of a Receiving Operating Characteristics curve that
302 assesses the performance of a binary classifier comparing the true and false positive
303 rates. We used historical changes as observed and changes predicted by our model as
304 expected.

305

306 **3. Results**

307 3.1. Influence of anthropogenic impact on body mass distribution

308 The best models for median and maximum body mass (Table 1, Table S5) included
309 one or two of the human impact variables considered. Travel time from major cities (a
310 proxy of accessibility to humans) showed a positive relationship with median and
311 maximum body mass, indicating that larger species tend to inhabit more inaccessible
312 areas (Table 2; Table S6). Similarly, median body mass decreased with increasing
313 time from first land use, indicating that larger mammals are found in more pristine
314 areas. Maximum body mass was lower in islands than in mainland.

315 We found similar results for skewness in body mass distribution. For this variable no
316 model was unequivocally supported ($\omega > 0.9$). The three most supported models
317 ($\omega > 0.1$) included accessibility, percentage of agricultural area, time from first land
318 use, and the factor island (Table 1; Table S5). Skewness increased with increasing
319 percentage of agricultural areas and time from first land use, and decreased with
320 increasing travel time from major cities. In islands skewness was lower (Table 1;
321 Table S6). Qualitatively similar results were found using AIC for model selection
322 (Table S7).

323

324 3.2. Alteration of body mass distribution pattern

325 The relationship between latitude and median body mass (Bergmann's rule) is
326 negative in the northern hemisphere above 20°N and in the southern hemisphere, but
327 positive between 0° and 20°N. Conversely, the relationship between latitude with
328 maximum body mass was positive with latitude above 20°N and slightly positive in
329 the southern hemisphere, and slightly negative between 0° and 20°N. The slopes

330 decreased in the northern hemisphere above 20° with human impact for median and
331 maximum body mass, increased between 0° and 20°, and decreased for the Southern
332 hemisphere for both median and maximum body mass (Table 2; Fig. 2).

333 Comparing the best model predictions under the two scenarios, we estimated
334 that under the minimal human impacts scenario we would expect an increase of 123.9
335 ± 37.4 g (mean \pm SD) in median body mass and of 9.9 ± 2.4 kg in maximum body
336 mass, corresponding to a relative increase of 22.4 ± 5.7 % and 25.6 ± 6.2 %
337 respectively (Fig. 3). For mainlands, median and maximum body mass loss were
338 particularly noticeable in United States, Southeastern Brazil, Europe, Sub-Saharan
339 Africa, Central and South East Asia, and Southern east and west Australia. In general
340 islands showed lower absolute losses, but similar relative values (Fig. 3).

341

342 3.3. Comparison with historical dataset

343 Our results were generally consistent with estimates based on current and historical
344 data, although historical data suggested larger changes than our predictions in general,
345 but negative changes in the Amazon basin and Australia (Fig. S3). We calculated
346 AUC values of 0.51 and 0.71 for the mean and maximum body mass respectively
347 indicating no and moderate agreement in change tendency.

348

349 **4. Discussion**

350 4.1. Alteration of body mass distribution pattern

351 Our results indicate that the present values of mammalian body mass are lower than
352 those expected under “natural” environmental conditions alone. Current body mass
353 distribution in terrestrial mammal assemblages appeared largely influenced by
354 existing human impacts. In particular, high body mass values were associated with

355 remote areas (those requiring longer travel times from major cities), lower human
356 population density and with no or recent land conversion. Human population density
357 and accessibility can be considered proxies of many human disturbance factors
358 including over-exploitation from hunting and persecution (Nelson, 2008). Conversion
359 to agriculture has direct effects on local extinctions, by replacing natural habitat with
360 lands unsuitable to most species. Our analyses showed that both current and past
361 conversion can be relevant. Importantly, models including descriptors of human
362 impacts were more supported than the null models based only on “natural” conditions,
363 indicating that anthropogenic effects must be considered when trying to understand
364 current macroecological patterns.

365 Our results showed that the relationship between latitude and body mass,
366 (Bergmann’s rule) has been altered during the “Anthropocene”. We observed a
367 vertical shift in the relationship due to a widespread reduction in median and
368 maximum body mass. Noticeably, the shape of the relationship did not conform well
369 to the expectations derived from the Bergmann’s rule, and the slopes were altered by
370 human impact at the three different latitudinal belts (>20° of latitude in the northern
371 hemisphere, between 0° and 20°N, and southern hemisphere), which could reflect an
372 unequal latitudinal intensity of human pressure. The presence of species with different
373 sensibilities (Fritz et al., 2009) is also likely responsible for this observed difference.
374 This result obtained through a statistical approach agrees with that obtained by Faurby
375 & Araujo (2016) that looked at the comparison between current and historical ranges.

376 Under the minimal human impact scenario, the largest absolute increase of
377 body mass was predicted in northern temperate areas, Sub-Saharan Africa and South-
378 East Asia, whereas when expressed as relative increase it was more evenly
379 distributed. These changes likely reflect distinct processes. The difference between

380 expected and observed body mass might reflect the loss of megafauna that occurred
381 during the late-Pleistocene and Holocene (Lister & Stuart, 2007; Barnosky &
382 Lindsey, 2010; Woinarski et al., 2015). Yet, it is likely that our model mostly captures
383 more recent impacts. In northern temperate areas large species have disappeared in
384 historical times, such as the auroch (*Bos primigenius*) and the tarpan (*Equus ferus*
385 *ferus*), while others have largely contracted their ranges, especially ungulates and
386 carnivores. Africa hosts the largest mammalian fauna today, although populations of
387 African mammals have declined substantially in recent times due to human impacts
388 (Craigie et al., 2010; Di Marco et al., 2014b), and many large species such as the
389 African elephant (*Loxodonta africana*) or the white rhino (*Ceratotherium simum*)
390 have suffered recent and severe range contractions (Ripple et al., 2014, 2015; IUCN,
391 2015). India and Southeast Asia have also experienced widespread range contractions
392 and the loss of some large-bodied species recently due to the interactive effect of
393 unsustainable hunting, habitat degradation, and more recently illegal wildlife trade
394 (Sodhi et al., 2004; Corlett, 2007).

395

396 4.2. Potential limitations of our approach

397 The comparison of our approach with estimates based on historical distribution ranges
398 showed some diverse results for median and maximum body mass. Median body mass
399 showed no agreement with historical data, whereas maximum body mass showed
400 moderate agreement but also highlighted regional variation. The difference in median
401 body mass can be attributed to the large areas in which median body mass is predicted
402 to have increased by historical data (Fig. S3). This can be caused by the recent loss of
403 small species that is not captured by our model, which is mostly influenced by areas
404 in which large mammals have decreased. Assemblage-level analyses are indeed more

405 influenced by large species as these are more widely distributed than smaller species
406 (Slavenko & Meiri, 2015). Regional differences between the approaches may occur
407 because of limitations in our approach, only based on current data, but also because of
408 limitations in the historical dataset. In fact, although we treated the data derived from
409 the historical dataset as “observed data”, these are necessarily associated to the level
410 of information available, and are a coarse representation of past species distributions.
411 Yet, by using a different approach we reached the same conclusion of Faurby &
412 Araújo (2016) that humans have distorted body mass distributions in mammal
413 assemblages.

414 One of the limitations in our dataset is that we could not account for the effect
415 of historical over-exploitation, which has likely driven many species to extinction
416 (Faurby & Svenning, 2015; Bartlett et al., 2016). Another potential limitation of our
417 analyses is that we used some environmental variables (e.g., evapotranspiration and
418 primary productivity) that likely reflect human impacts indirectly via habitat
419 modification (fire regimes and agriculture) and climate change. Thus, the minimal
420 impact scenario does not represent pristine conditions, and this makes our estimates of
421 body mass reduction conservative. On the other hand, past extinctions also reflect
422 changes in environmental conditions, not just human impacts, so not all changes in
423 body mass distribution may have been caused by human actions. For example, it is
424 still debated whether early Pleistocene extinctions are to be attributed to climate
425 change, human impact or the combined effect of both (see Koch & Barnosky, 2006;
426 Araujo et al., 2015; Cooper et al., 2015; Bartlett et al., 2016). Similarly, elevation
427 range was used as environmental predictor of mesoscale climatic variation and
428 environmental heterogeneity following previous work (Rodríguez et al., 2006;
429 Rodríguez et al., 2008; Diniz-Filho et al., 2009; Olson et al., 2009). Yet areas with

430 high range of elevation are also likely less accessible to humans, and therefore may
431 also act as a proxy of human impact. Nevertheless, the main scope of our approach is
432 heuristic rather than predictive, and its merit is to illustrate the potential to assess the
433 relative contribution of recent human impact in altering the body mass of mammal
434 species assemblages, and to highlight the need for considering human impact
435 variables to understand macroecological patterns.

436

437 4.3. Conclusion

438 Current body mass distribution is the result of the interaction between natural and
439 anthropogenic factors. Macroecological investigation has traditionally focused on the
440 underlying environmental predictors of natural patterns, but we live in an era of rapid
441 global change. Neglecting the effect of human impact on global macroecological
442 patterns can lead to misleading conclusions on the underlying causes of species
443 distribution (Diniz-Filho et al., 2009; Di Marco & Santini, 2015a; Torres-Romero &
444 Olalla-Tárraga, 2015). Although in many cases macroecological studies are only
445 interested in the underlying environmental predictors of natural patterns, neglecting
446 human impact can lead to misrepresentations and potentially biased estimates of the
447 relative contribution of environmental variables. In fact, human impact and
448 environmental conditions are partly correlated (Table S1), since the former includes
449 processes such as agricultural intensification, urbanisation, and deforestation, which
450 are dependent upon the environmental context. There is a risk that a given
451 environmental variable is found to be a good macroecological predictor, while in fact
452 it is just a distal proxy of suitability for human activities.

453 Since the ecological determinants of local extinctions may be extremely slow
454 to manifest, being barely noticed in a lifetime, macroecological studies are at risk of

455 incorrectly assuming that the large-scale patterns that we observe today are
456 sufficiently close to pristine natural conditions. In a sense, this may extend the notion
457 of “shifting baseline syndrome” (Papworth et al., 2009) to “shifting macroecological
458 baseline”: when the first macroecological investigations started, our understanding of
459 global geographic patterns was based on a situation which was already compromised.
460 Incorporating anthropogenic variables into statistical models of macroecological
461 patterns may permit to account for this issue. However, this is unlikely to completely
462 wipe out the effect of humans from the patterns, due to the inherent difficulty in
463 representing some specific (e.g. hunting) and/or prehistorical human impacts. An
464 informed interpretation that considers possible alterations from the original condition
465 is ultimately necessary.

466

467 **Acknowledgements**

468 We thank Luigi Maiorano, Francesco Ficetola, Miguel Olalla-Tárraga, Søren Faurby,
469 Jens-Christian Svenning, Yolanda Wiersma and an anonymous reviewer for providing
470 constructive comments that improved the manuscript.

471

472 **References**

- 473 Adams D.C. & Church J.O. (2011) The evolution of large-scale body size clines in
474 *Plethodon* salamanders: evidence of heat-balance or species-specific artifact?
475 *Ecography*, **34**, 1067–1075.
- 476 Allendorf F.W. & Hard J.J. (2009) Human-induced evolution caused by unnatural
477 selection through harvest of wild animals. *Proceedings of the National Academy
478 of Sciences of the United States of America*, **106 Suppl**, 9987–9994.
- 479 Amante C. & Eakins B.W. (2009) ETOPO1 1 Arc-Minute Global Relief Model:

480 Procedures, Data Sources and Analysis. *NOAA Technical Memorandum NESDIS*
481 *NGDC-24. National Geophysical Data Center, NOAA, .*

482 Araujo B.B.A., Oliveira-Santos L.G.R., Lima-Ribeiro M.S., Diniz-Filho J.A.F., &
483 Fernandez F.A.S. (2015) Bigger kill than chill: The uneven roles of humans and
484 climate on late Quaternary megafaunal extinctions. *Quaternary International, .*

485 Barnosky A.D. & Lindsey P.A. (2010) Timing of Quaternary megafaunal extinction
486 in South America in relation to human arrival and climate change. *Quaternary*
487 *International, 217*, 10–29.

488 Bartlett L.J., Williams D.R., Prescott G.W., Balmford A., Green R.E., Eriksson A.,
489 Valdes P.J., Singarayer J.S., & Manica A. (2016) Robustness despite uncertainty:
490 regional climate data reveal the dominant role of humans in explaining global
491 extinctions of Late Quaternary megafauna. *Ecography, 39*, 152–161.

492 Bergmann C. (1847) Über die Verhältnisse der Wärmeökonomie der Thiere zu ihrer
493 Grösse. *Gottinger studien, 3*, 595–708.

494 Blackburn T.M., Gaston K.J., & Loder N. (1999) Geographic gradients in body size: a
495 clarification of Bergmann’s rule. *Diversity and Distributions, 5*, 165–174.

496 Blackburn T.M. & Hawkins B.A. (2004) Bergmann’s rule and the mammal fauna of
497 northern North America. *Ecography, 27*, 715–724.

498 Brown J.H. & Lee A.K. (1969) Bergmann’s rule and climatic adaptation in woodrats
499 (Neotoma). *Evolution, 23*, 329–338.

500 Burnham K.P. & Anderson D.R. (2002) *Model Selection and Multimodel Inference: A*
501 *Practical Information-Theoretic Approach*. Springer, New York.

502 Calder W.A. (1984) *Size, function and life history*. Harvard University Press,
503 Cambridge, Mass.

504 Cardillo M., Mace G.M., Jones K.E., Bielby J., Bininda-Emonds O.R.P., Sechrest W.,

505 Orme C.D.L., & Purvis A. (2005) Multiple causes of high extinction risk in large
506 mammal species. *Science*, **309**, 1239–1241.

507 CIESIN & CIAT (2005) Gridded Population of the World, Version 3 (GPWv3):
508 Population Density Grid. NASA Socioeconomic Data and Applications Center
509 (SEDAC), Palisades, NY. .

510 Cooper A., Turney C., Hughen K.A., Brook B.W., McDonald H.G., & Bradshaw
511 C.J.A. (2015) Abrupt warming events drove Late Pleistocene Holarctic
512 megafaunal turnover. *Science*, **349**, 602–606.

513 Corlett R. (2007) The impact of hunting on the mammalian fauna of tropical Asian
514 forests. *Biotropica*, **39**, 292–303.

515 Craigie I.D., Baillie J.E.M., Balmford A., Carbone C., Collen B., Green R.E., &
516 Hutton J.M. (2010) Large mammal population declines in Africa’s protected
517 areas. *Biological Conservation*, **143**, 2221–2228.

518 Damuth J. (1981) Population density and body size in mammals. *Nature*, **290**, 699–
519 700.

520 Di Marco M., Boitani L., Mallon D., Hoffmann M., Iacucci A., Meijaard E., Visconti
521 P., Schipper J., & Rondinini C. (2014a) A retrospective evaluation of the global
522 decline of carnivores and ungulates. *Conservation Biology*, **28**, 1109–1118.

523 Di Marco M., Buchanan G.M., Szantoi Z., Holmgren M., Grotto Marasini G., Gross
524 D., Tranquilli S., Boitani L., & Rondinini C. (2014b) Drivers of extinction risk in
525 African mammals: the interplay of distribution state, human pressure,
526 conservation response and species biology. *Philosophical Transactions of the
527 Royal Society of London B Biological Sciences*, **369**, 20130198.

528 Di Marco M., Collen B., Rondinini C., & Mace G. (2015) Historical drivers of
529 extinction risk: using past evidence to direct future monitoring. *Proceedings of*

530 *the Royal Society B*, **282**, 20150928.

531 Di Marco M. & Santini L. (2015a) Human pressures predict species' geographic
532 range size better than biological traits. *Global Change Biology*, **21**, 2169–2178.

533 Di Marco M. & Santini L. (2015b) Climatic tolerance or geographic breadth: what are
534 we measuring? *Global Change Biology*, **22**, 972–973.

535 Diniz-Filho J.A.F., Rodríguez M.A., Bini L.M., Olalla-Tarraga M.A., Cardillo M.,
536 Nabout J.C., Hortal J., & Hawkins B.A. (2009) Climate history, human impacts
537 and global body size of Carnivora (Mammalia: Eutheria) at multiple evolutionary
538 scales. *Journal of Biogeography*, **36**, 2222–2236.

539 Diniz-Filho J.A.F., de Sant'Ana C.E.R., & Bini L.M. (1998) An Eigenvector Method
540 for Estimating Phylogenetic Inertia. *Evolution*, **52**, 1247–1262.

541 Dirzo R., Young H.S., Galetti M., Ceballos G., Isaac N.J.B., & Collen B. (2014)
542 Defaunation in the Anthropocene. *Science*, **345**, 401–406.

543 Dunbrack R.L. & Ramsay M.A. (1993) The allometry of mammalian adaptations to
544 seasonal environments: a critique of the fasting endurance hypothesis. *Oikos*, **66**,
545 336–342.

546 Ellis E.C., Kaplan J.O., Fuller D.Q., Vavrus S., Goldewijk K.K., & Verburg P.H.
547 (2013) Used planet: A global history. *Proceedings of the National Academy of*
548 *Sciences*, **110**, 7978–7985.

549 Faurby S. & Araújo M.B. (2016) Anthropogenic impacts weaken Bergmann's rule.
550 *Ecography*, .

551 Faurby S. & Svenning J. (2016) Resurrection of the Island Rule: Human-Driven
552 Extinctions Have Obscured a Basic Evolutionary Pattern. *The American*
553 *Naturalist*, **187**, 812–820.

554 Faurby S. & Svenning J.C. (2015) Historic and prehistoric human-driven extinctions

555 have reshaped global mammal diversity patterns. *Diversity and Distributions*, **21**,
556 1155–1166.

557 Fenchel T. (1974) Intrinsic Rate of Natural Increase: The Relationship with Body
558 Size. *Oecologia*, **14**, 317–326.

559 Freckleton R.P., Cooper N., & Jetz W. (2011) Comparative Methods as a Statistical
560 Fix: The Dangers of Ignoring an Evolutionary Model. **178**, E10–E17.

561 Fritz S.A., Bininda-Emonds O.R.P., & Purvis A. (2009) Geographical variation in
562 predictors of mammalian extinction risk: Big is bad, but only in the tropics.
563 *Ecology Letters*, **12**, 538–549.

564 Goodman S.M., Rasoloarison R.M., & Ganzhorn J.U. (2004) On the specific
565 identification of subfossil Cryptoprocta (Mammalia, Carnivora) from
566 Madagascar. *Zoosystema*, **26**, 129–143.

567 Hijmans R.J., Cameron S.E., Parra J.L., Jones P.G., & Jarvis A. (2005) Very high
568 resolution interpolated climate surfaces for global land areas. *International*
569 *Journal of Climatology*, **25**, 1965–1978.

570 IONIA (2009) Globcover land cover. See <http://ionia1.esrin.esa.int> . .

571 IUCN (2015)

572 James F.C. (1970) Geographic size variation in birds and its relationship to climate.
573 *Ecology*, **51**, 365–390.

574 Johnson C.N. (2002) Determinants of loss of mammal species during the Late
575 Quaternary “megafauna” extinctions: life history and ecology, but not body size.
576 *Proceedings of the Royal Society B*, **269**, 2221–2227.

577 Jones K.E., Bielby J., Cardillo M., Fritz S.A., O’Dell J., Orme C.D.L., Safi K.,
578 Sechrest W., Boakes E.H., Carbone C., Connolly C., Cutts M.J., Foster J.K.,
579 Grenyer R., Habib M., Plaster C.A., Price S.A., Rigby E.A., Rist J., Teacher A.,

580 Bininda-Emonds O.R.P., Gittleman J.L., Mace G.M., Purvis A., & Michener
581 W.K. (2009) PanTHERIA: a species-level database of life history, ecology, and
582 geography of extant and recently extinct mammals. *Ecology*, **90**, 2648.

583 Kissling W.D. & Carl G. (2008) Spatial autocorrelation and the selection of
584 simultaneous autoregressive models. *Global Ecology and Biogeography*, **17**, 59–
585 71.

586 Koch P.L. & Barnosky A.D. (2006) Late Quaternary Extinctions: State of the Debate.
587 *Annual Review of Ecology and Systematics*, **37**, 215–250.

588 Legendre P. & Legendre L. (1998) Numerical ecology. *Numerical Ecology Second*
589 *English Edition*, **20**, 870.

590 Lewin-Koh N. & Bivand R. (2011) maptools: Tools for reading and handling spatial
591 objects. *R package version ...*, 74.

592 Lindstedt S.L. & Boyce M.S. (1985) Seasonality, fasting endurance, and body size in
593 mammals. *American Naturalist*, **125**, 873–878.

594 Lister A. & Stuart A.J. (2007) Patterns of Late Quaternary megafaunal extinctions in
595 Europe and northern Asia. *Courier Forschungsinstitut Senckenberg*, **259**, 289–
596 299.

597 Lyons S.K., Smith F.A., & Brown J.H. (2004) Of mice, mastodons and men: Human-
598 mediated extinctions on four continents. *Evolutionary Ecology Research*, **6**, 339–
599 358.

600 MacPhee R.D.E. & Grimaldi D.A. (1996) Mammal bones in Dominican amber.
601 *Nature*, **380**, 489–490.

602 Maurer B. a, Brown J.H., & Rusler R.D. (1992) The Micro and Macro in Body Size
603 Evolution. *Evolution*, **46**, 939–953.

604 McNab B.K. (2010) Geographic and temporal correlations of mammalian size

605 reconsidered: A resource rule. *Oecologia*, **164**, 13–23.

606 Meiri S. (2011) Bergmann’s Rule – what’s in a name? *Global Ecology and*
607 *Biogeography*, **20**, 203–207.

608 Meiri S. & Thomas G.H. (2007) The geography of body size – challenges of the
609 interspecific approach. *Global Ecology and Biogeography*, **16**, 689–693.

610 Milner-Gulland E.J. & Bennet E.L. (2003) Wild meat: the bigger picture. *Trends in*
611 *Ecology & Evolution*, **18**, 351–357.

612 Morales-Castilla I., Olalla-Tárraga M.Á., Purvis A., Hawkins B. a., & Rodríguez
613 M.Á. (2012) The Imprint of Cenozoic Migrations and Evolutionary History on
614 the Biogeographic Gradient of Body Size in New World Mammals. *The*
615 *American Naturalist*, **180**, 246–256.

616 Morrison J.C., Sechrest W., Dinerstein E., Wilcove D.S., & Lamoreux J.F. (2007)
617 Persistence of large mammal faunas as indicators of global human impacts.
618 *Journal of Mammalogy*, **88**, 1363–1380.

619 Murray B.R. & Dickman C.R. (2000) Relationships between body size and
620 geographical range size among Australian mammals: has human impact distorted
621 macroecological patterns? *Ecography*, **23**, 92–100.

622 Nelson A. (2008) Travel Time to Major Cities: A Global Map of Accessibility.
623 *Global Environment Monitoring Unit – Joint Research Centre of the European*
624 *Commission, Ispra, Italy.*, .

625 Newbold T., Hudson L.N., Arnell A.P., Contu S., Palma A.D., Ferrier S., Hill S.L.L.,
626 Hoskins A.J., Lysenko I., Phillips H.R.P., Burton V.J., Chng C.W.T., Emerson
627 S., Gao D., Pask-Hale G., Hutton J., Jung M., Sanchez-Ortiz, K., Simmons B.I.,
628 Whitmee S., & Zhang H. (2016) Has land use pushed terrestrial biodiversity
629 beyond the planetary boundary? A global assessment. *Science*, **353**, 288–291.

630 Olalla-Tárraga M.A., Torres-Romero E.J., Amado T.F., & Martínez P.A. (2015)
631 Phylogenetic path analysis reveals the importance of niche-related biological
632 traits on geographic range size in mammals. *Global Change Biology*, **21**, 3194–
633 3196.

634 Olalla- Tárraga M.Á., Bini L.M., Diniz- Filho J.A., & Rodríguez M.Á. (2010)
635 Cross- species and assemblage- based approaches to Bergmann’s rule and the
636 biogeography of body size in Plethodon salamanders of eastern North America.
637 *Ecography*, **33**, 362–368.

638 Olson V.A., Davies R.G., Orme D.L., Thomas G.H., Meiri S., Blackburn T.M.,
639 Gaston K.J., Owens I.P.F., & Bennett P.M. (2009) Global biogeography and
640 ecology of body size in birds. *Ecology Letters*, **12**, 249–259.

641 Pacifici M., Santini L., Di Marco M., Baisero D., Francucci L., Grottolo Marasini G.,
642 Visconti P., & Rondinini C. (2013) Generation length for mammals. *Nature*
643 *Conservation*, **5**, 87–94.

644 Papworth S.K., Rist J., Coad L., & Milner-Gulland E.J. (2009) Evidence for shifting
645 baseline syndrome in conservation. *Conservation Letters*, **2**, 93–100.

646 Purvis A., Agapow P.M., Gittleman J.L., & Mace G.M. (2000) Nonrandom Extinction
647 and the Loss of Evolutionary History. *Science*, **288**, 328–330.

648 R Core Team (2016) R: A language and environment for statistical computing. *R*
649 *Foundation for Statistical Computing, Vienna, Austria. [http://www.R-](http://www.R-project.org/)*
650 *project.org/*, .

651 Raffalovich L.E., Deane G.D., Armstrong D., & Tsao H.-S. (2008) Model selection
652 procedures in social research: Monte-Carlo simulation results. *Journal of Applied*
653 *Statistics*, **35**, 1093–1114.

654 Ripple W.J., Estes J.A., Beschta R.L., Wilmers C.C., Ritchie E.G., Hebblewhite M.,

655 Berger J., Elmhagen B., Letnic M., Nelson M.P., Schmitz O.J., Smith D.W.,
656 Wallach A.D., & Wirsing A.J. (2014) Status and Ecological Effects of the
657 World's Largest Carnivores. *Science*, **343**, 1241484.

658 Ripple W.J., Newsome T.M., Wolf C., Dirzo R., Everatt K.T., Galetti M., Hayward
659 M.W., Kerley G.I.H., Levi T., Lindsey P.A., Macdonald D.W., Malhi Y., Painter
660 L.E., Sandom C.J., Terborgh J., & Van Valkenburgh B. (2015) Collapse of the
661 world's largest herbivores. *Science Advances*, **1**, e1400103.

662 Ripple W.J. & Van Valkenburgh B. (2010) Linking Top-down Forces to the
663 Pleistocene Megafaunal Extinctions. *BioScience*, **60**, 516–523.

664 Rodríguez M.A., López-Sañudo I.L., & Hawkins B.A. (2006) The geographic
665 distribution of mammal body size in Europe. *Global Ecology and Biogeography*,
666 **15**, 173–181.

667 Rodríguez M.A., Olalla-Tárraga M.A., & Hawkins B.A. (2008) Bergmann's rule and
668 the geography of mammal body size in the Western Hemisphere. *Global Ecology
669 and Biogeography*, **17**, 274–283.

670 Slavenko A. & Meiri S. (2015) Mean body sizes of amphibian species are poorly
671 predicted by climate. *Journal of Biogeography*, 1246–1254.

672 Smith F.A., Lyons K., Morgan Ernest S.K., Jones K.E., Kaufman D.M., Dayan T.,
673 Marquet P.A., Brown J.H., & Haskell J.P. (2003) Body mass of late quaternary
674 mammals. *Ecology*, **84**, 3403–3403.

675 Smith F.A. & Lyons S.K. (2011) How big should a mammal be? A macroecological
676 look at mammalian body size over space and time. *Philosophical Transactions of
677 the Royal Society of London B Biological Sciences*, **366**, 2364–2378.

678 Sodhi N.S., Koh L.P., Brook B.W., & Ng P.K.L. (2004) Southeast Asian biodiversity:
679 An impending disaster. *Trends in Ecology and Evolution*, **19**, 654–660.

680 Speakman J.R. & Król E. (2010) Maximal heat dissipation capacity and hyperthermia
681 risk: neglected key factors in the ecology of endotherms. *Journal of Animal*
682 *Ecology*, **79**, 726–746.

683 Torres-Romero E.J. & Olalla-Tárraga M.A. (2015) Untangling human and
684 environmental effects on geographical gradients of mammal species richness: a
685 global and regional evaluation. *Journal of Animal Ecology*, **84**, 851–860.

686 Villalobos F., Olalla-Tárraga M.Á., Cianciaruso M. V., Rangel T.F., & Diniz-Filho
687 J.A.F. (2016) Global patterns of mammalian co-occurrence: phylogenetic and
688 body size structure within species ranges. *Journal of Biogeography*, 1–11.

689 van Vuure C. (2005) *Retracing the aurochs: history, morphology and ecology of an*
690 *extinct wild ox*. Pensoft, Sofia-Moscow.

691 Woinarski J.C., Burbidge A.A., & Harrison P.L. (2015) Ongoing unraveling of a
692 continental fauna: Decline and extinction of Australian mammals since European
693 settlement. *Proceedings of the National Academy of Sciences*, **112**, 4531–4540.

694 Woodroffe R. (2000) Predators and people: using human densities to interpret
695 declines of large carnivores. *Animal Conservation*, **3**, 165–173.

696

Table 1. Comparison of SAR models explaining the observed distribution of median (Med), maximum body mass represented as the 90th percentile (Max) and body mass skewness (Skew). Only the most supported models are shown here ($\omega \geq 0.1$; see Table S5 for all models). df = degree of freedom; BIC = Bayesian Information Criterion; Δ BIC = difference in BIC with the best model; ω = BIC weight; R^2_{sp} = variance explained by the fixed factor and the spatial autocorrelation combined; R^2_{nsp} = variance explained by the fixed factors only. C1-2 = First two principal components explaining ~ 65% of the variance of environmental variables and order richness; Acc = Accessibility; pAg = Percentage of agricultural areas; PD = Population density; YFU = Year from first land use; ISL = factor to classify cells as islands (ISL1 = <25,000 km²; ISL2 = <100,000 km²; ISL3 = <500,000 km²; ISL4 = <750,000,000 km²).

Formula	df	BIC	Δ BIC	ω	R^2_{sp}	R^2_{nsp}	Int	C1	C2	Acc	YFU	pAg	ISL4
<i>Med ~ C1 + C2 + YFU + Acc</i>	7	-8564.03	0	0.95	0.94	0.08	-0.354 (0.019) *	0.011 (0.007)	-0.071 (0.011) *	0.032 (0.005) *	-0.017 (0.004) *	-	-
<i>Max ~ ISL4 + C1 + C2 + Acc</i>	7	-17291.36	0	0.94	0.92	0.17	1.466 (0.014) *	0.000 (0.005)	0.035 (0.009) *	0.037 (0.004) *	-	-	-0.183 (0.017) *
<i>Skew ~ ISL4 + C1 + C2 + YFU + Acc</i>	8	-39027.21	0	0.43	0.91	0.30	0.561 (0.005) *	-0.042 (0.002)*	-0.013 (0.004) *	-0.004 (0.002) *	0.003 (0.001)	-	-0.091 (0.007) *
<i>Skew ~ ISL4 + C1 + C2 + Acc + pAg</i>	8	-39026.66	0.54	0.33	0.91	0.30	0.561 (0.005) *	-0.042 (0.002) *	-0.012 (0.004) *	-0.004 (0.002) *	-	0.003 (0.002)	-0.091 (0.007) *
<i>Skew ~ ISL4 + C1 + C2 + Acc</i>	7	-39025.27	1.94	0.16	0.91	0.30	0.561 (0.005) *	-0.043 (0.002) *	-0.013 (0.004) *	-0.005 (0.002) *	-	-	-0.090 (0.007) *

Table 2. Difference (Δ) of the estimated coefficients and standard errors (in brackets) of intercepts and slopes describing the relationship between latitude and predicted body mass according to the two scenarios of human impact ($Body\ mass \sim Human_Impact + Latitude:Human_Impact$). $\Delta =$ Coefficient for the minimal impact scenario - Coefficient for the observed impact scenario; N = Northern hemisphere; S = Southern hemisphere; * = P-value <0.05 ; df = degree of freedom. Significance indicates a significant alteration of the relationship between latitude and body mass. Standard errors equal to zero are due to the rounding of the fourth decimal value.

Model	Δ Intercept	Δ Slope latitude
Med (Northern hemisphere)	0.214(0.003)*	-0.002(1×10^{-4})*
Med ($0^\circ - 20^\circ$)	0.123(0.004)*	0.002(3×10^{-4})*
Med (Southern hemisphere)	0.128(0.002)*	-4×10^{-4} (1×10^{-4})*
Max (Northern hemisphere)	12.670(0.121)*	-0.051(0.002)*
Max ($0^\circ - 20^\circ$)	8.752(0.127)*	0.049(0.011)*
Max (Southern hemisphere)	8.182(0.105)*	-0.070(0.005)*

Figures

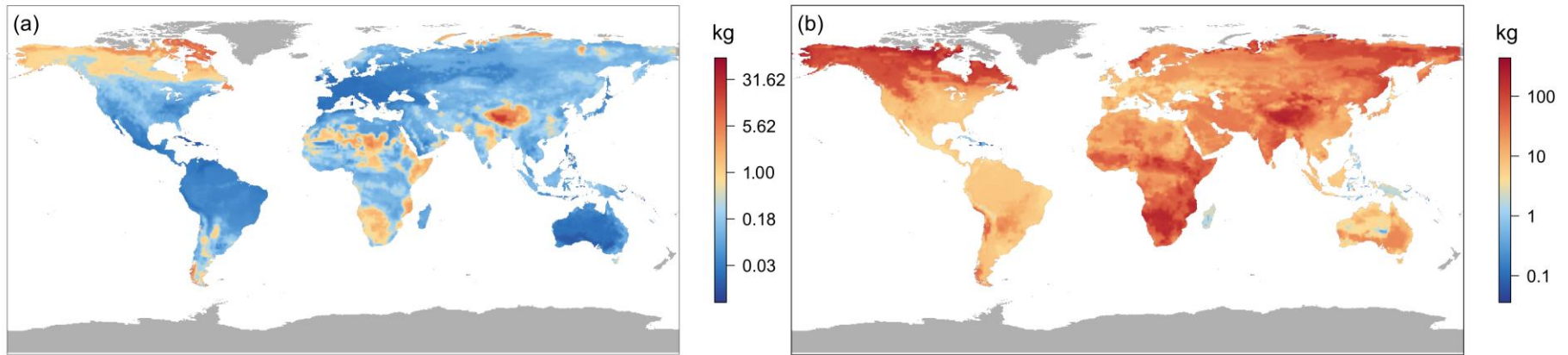


Fig. 1. Median (a) and maximum (b) values of body mass in terrestrial mammals (values on a log-10 scale aggregated into grids of 1 degree). Cells with ≤ 5 species are represented in grey (and were not considered in the analyses). The maximum is reported as the 90% percentile of the body mass distribution (only for cells with >10 species).

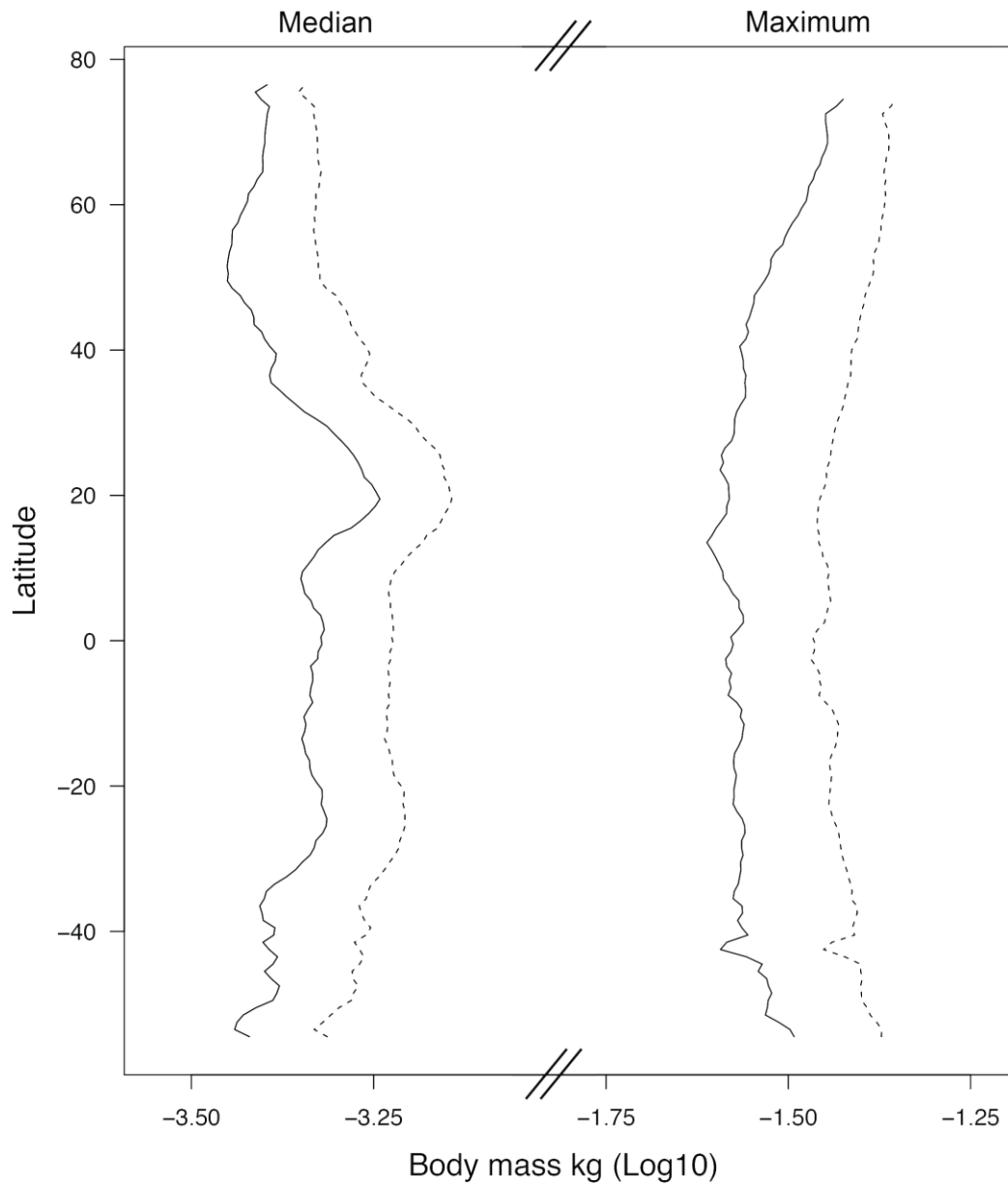


Fig. 2. Relationship between latitude and median and maximum body mass.

Continuous lines represent the predictions with human impact, whereas dashed lines the predictions without human impact.

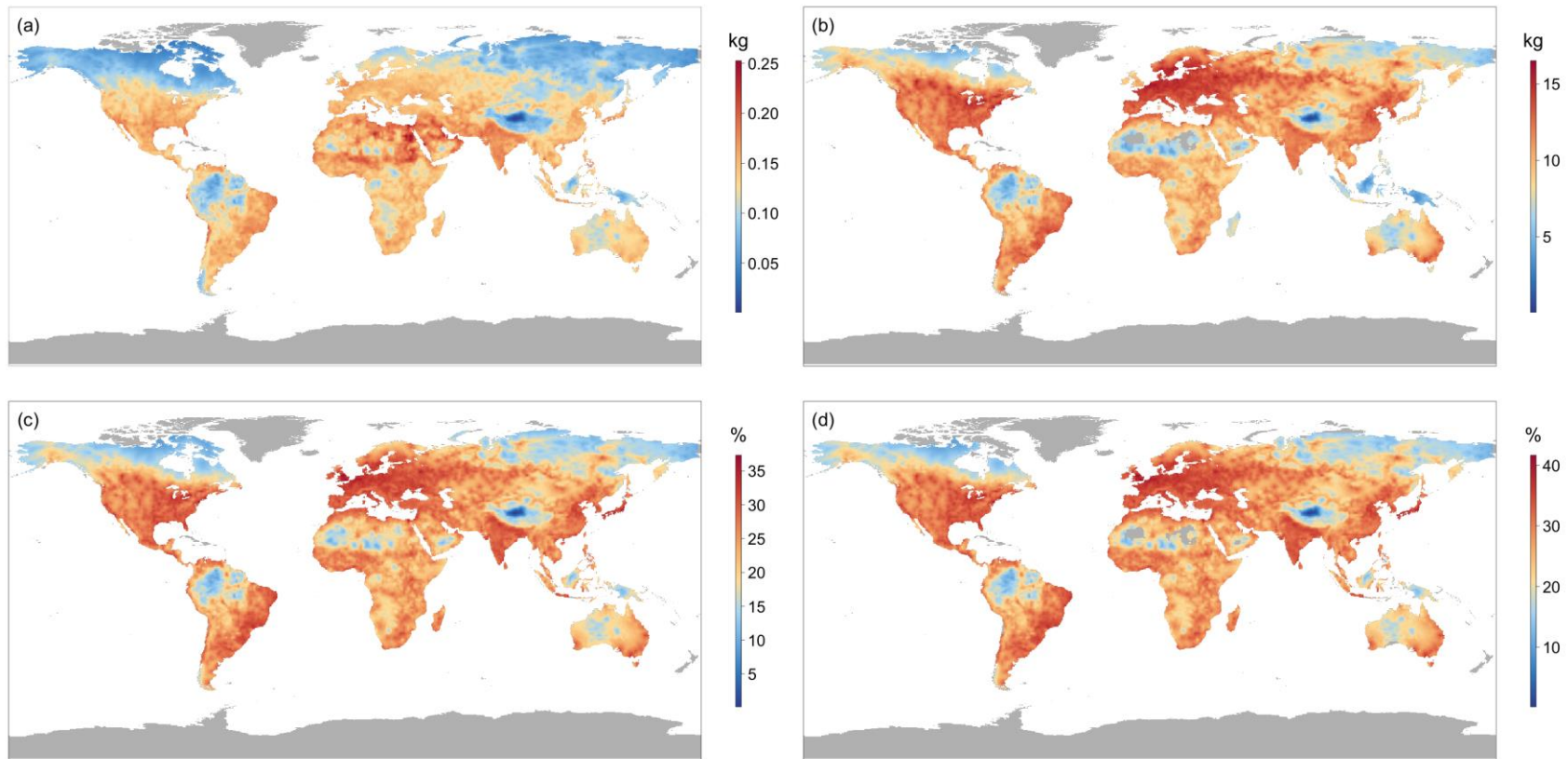


Fig. 3. Difference in predicted body mass between the observed and minimal impact scenarios. The plots report the absolute difference in median (a) and maximum (b) body mass values, and the relative (%) difference in median (c) and maximum (d) body mass values. Cells with ≤ 5 and ≤ 10 species are represented in grey for median and maximum respectively (and were not considered in the analyses).

SUPPORTING INFORMATION

Additional Supporting Information may be found in the online version of this article:

Table S1. Correlation matrix of all variables used in the study.

Table S2. Importance values and broken-stick distribution of the principal components.

Table S3. Loadings of variables on the principal components.

Table S4. Moran Index test results for OLS model's residuals.

Table S5. Comparison of models explaining the observed distribution of median, maximum body mass and body mass skewness based on BIC.

Table S6. Coefficient estimates for all models tested.

Table S7. Comparison of models explaining the observed distribution of median, maximum body mass and body mass skewness based on AIC.

Fig. S1. Correlograms for the null models of median and maximum body mass, and skewness in body mass distribution.

Fig. S2. Median (a) and maximum (b) values of body mass in terrestrial mammals estimated considering the historical geographic ranges from Faurby & Svenning (2015; values aggregated into grids of 1 degree, and log₁₀-transformed). The maximum is reported as the 97.5% percentile of the body mass distribution.

Fig. S3. Difference in median (a) and maximum (b) body mass between current and historical body mass distributions, estimated considering the historical geographic ranges from Faurby & Svenning (2015; values aggregated into grids of 1 degree, and log₁₀-transformed). Black areas are estimated to have increased mean and maximum body mass.

Biosketch

Luca Santini is a postdoctoral research fellow and his research primarily focuses on the link between macroecology and conservation biogeography, with main interests in species biological traits and their natural covariation, species distribution, patterns of spatial ecology, and the effect of anthropogenic impact in natural patterns.

Supplementary Materials

Shifting baseline in macroecology? Unraveling the influence of human impact on mammalian body mass

Luca Santini^{1,2*}, Manuela González-Suárez^{3,4}, Carlo Rondinini², Moreno Di Marco^{5,6}

¹ Department of Environmental Science, Radboud University, P.O. Box 9010, NL-6500 GL, Nijmegen, The Netherlands

² Global Mammal Assessment program, Department of Biology and Biotechnologies, Sapienza Università di Roma, Viale dell'Università 32, 00185 Rome, Italy

³ Department of Conservation Biology, Estación Biológica de Doñana - CSIC, 41092 Seville, Spain.

⁴ Ecology and Evolutionary Biology, School of Biological Sciences, University of Reading, Whiteknights, Reading, Berkshire, RG6 6AS, UK

⁵ ARC Centre of Excellence for Environmental Decision, Centre for Biodiversity and Conservation Science, The University of Queensland, St Lucia, QLD 4072 (Brisbane, Australia).

⁶ School of Earth and Environmental Sciences, The University of Queensland, St Lucia, QLD 4072 (Brisbane, Australia).

Fig. S1. Correlograms for the null models of (a) median and (b) maximum body mass, and (c) skewness in body mass distribution.

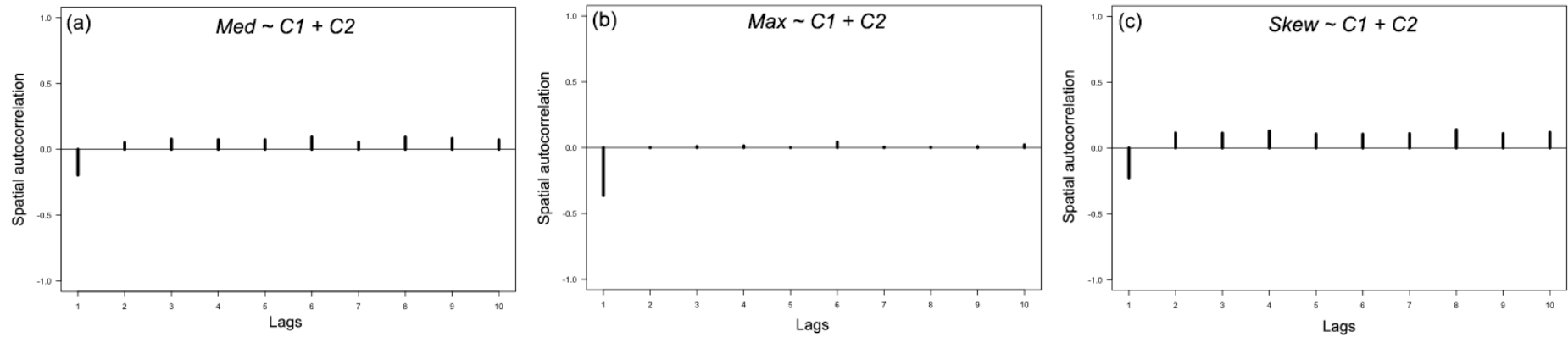


Fig. S2. Median (a) and maximum (b) values of body mass in terrestrial mammals estimated considering the historical geographic ranges from Faurby & Svenning (2015; values aggregated into grids of 1 degree, and log₁₀-transformed). The maximum is reported as the 97.5% percentile of the body mass distribution.

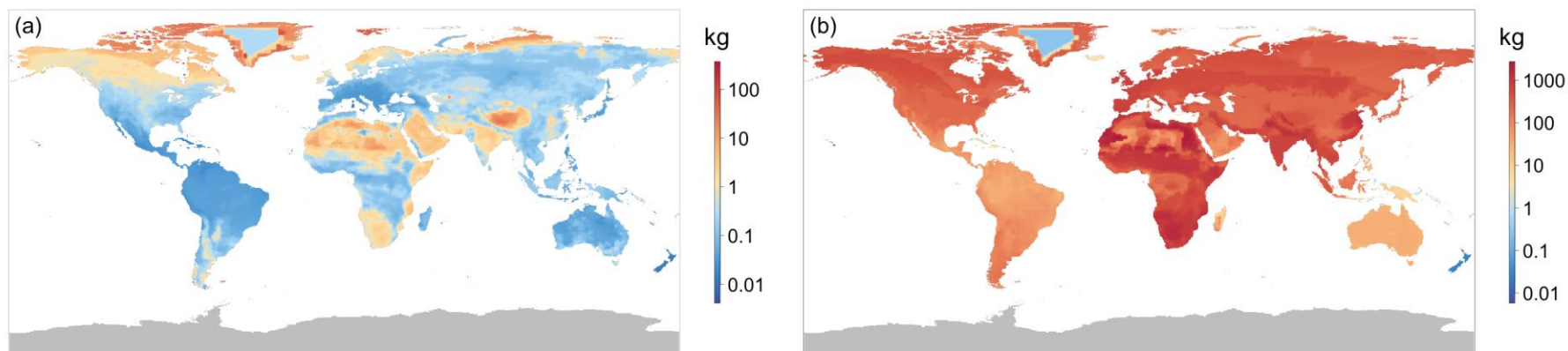


Fig. S3. Difference in median (a) and maximum (b) body mass between current and historical body mass distributions, estimated considering the historical geographic ranges from Faurby & Svenning (2015; values aggregated into grids of 1 degree, and log10- transformed). Black areas are estimated to have increased mean and maximum body mass.

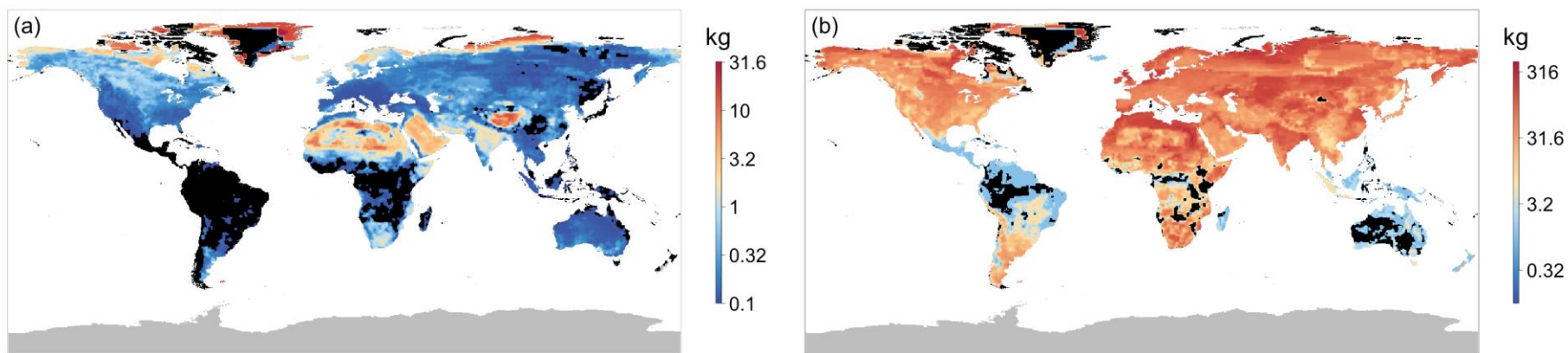


Table S1. Correlation matrix of all variables used in the study. pAg = Proportion of agricultural areas; PD = Population density; Acc = Accessibility; YFU = Year from first land use; Rich_O = Order richness; T = Mean annual temperature; Tcq = Mean temperature of the coldest quarter; Twq = Mean temperature of the warmest quarter; P = Mean annual precipitations; Pwq = Precipitations of the warmest quarter; Pdq = Precipitations of the driest quarter; TGR = Time since last glacial retreat; ER = Elevation range; NDVI = Normalized Difference of Vegetation Index; NDVI_cv = Within year coefficient of variation of the Normalized Difference of Vegetation Index; AET = Actual evapotranspiration; PET = Potential evapotranspiration. Correlation coefficients higher than 0.6 (or lower than -0.6) are highlighted in bold.

	pAg	PD	Acc	YFU	Rich_O	T	Tcq	Twq	P	Pwq	Pdq	TGR	ER	NDVI	NDVI_cv
PD	0.71														
Acc	-0.68	-0.74													
YFU	0.73	0.66	-0.70												
Rich_O	0.49	0.48	-0.31	0.44											
T	0.48	0.59	-0.41	0.42	0.59										
Tcq	0.49	0.58	-0.39	0.42	0.62	0.98									
Twq	0.38	0.55	-0.41	0.37	0.46	0.93	0.85								
P	0.4	0.25	-0.24	0.34	0.45	0.09	0.16	-0.07							
Pwq	0.42	0.29	-0.22	0.36	0.50	0.15	0.22	-0.01	0.98						
Pdq	0.15	-0.04	-0.09	0.1	0.03	-0.3	-0.24	-0.4	0.64	0.53					
TGR	0.39	0.56	-0.28	0.3	0.32	0.47	0.42	0.52	-0.02	0.03	-0.18				
ER	0.16	0.17	-0.04	0.12	0.05	-0.06	-0	-0.18	0.11	0.13	0.13	0.08			
NDVI	0.22	0.14	-0.17	0.19	0.26	-0.14	-0.1	-0.23	0.68	0.65	0.56	-0.07	-0.02		
NDVI_cv	0.39	0.24	-0.39	0.41	0.25	-0.06	-0.03	-0.15	0.58	0.56	0.45	-0.12	0.05	0.65	
AET	0.26	0.23	-0.17	0.24	0.38	0.16	0.16	0.13	0.39	0.41	0.18	0.15	-0.03	0.32	0.23

Table S2. Importance values and broken-stick distribution of the principal components. PCA components with larger percentages of accumulated variance than the broken-stick variances are significant (Legendre and Legendre, 1998).

	Comp.1	Comp.2	Comp.3	Comp.4	Comp.5	Comp.6	Comp.7	Comp.8	Comp.9	Comp.10	Comp.11	Comp.12
Eigenvalue	3.99	3.72	1.07	0.83	0.66	0.57	0.42	0.34	0.28	0.10	0.01	0.00
Standard deviation	2.00	1.93	1.04	0.91	0.81	0.75	0.65	0.58	0.53	0.31	0.11	0.03
% of Variance	33.26	31.03	8.96	6.88	5.51	4.75	3.53	2.84	2.35	0.79	0.10	0.01
Cumulative %	33.26	64.29	73.25	80.13	85.64	90.38	93.92	96.75	99.10	99.90	99.99	100.00
Broken-stick %	25.86	17.53	13.36	10.58	8.50	6.83	5.44	4.25	3.210	2.29	1.45	0.69
Broken-stick cumulative %	25.86	43.39	56.75	67.33	75.83	82.66	88.10	92.36	95.57	97.85	99.31	100.00

Table S3. Loadings of variables on the principal components (C).

	C1	C2	C3	C4	C5	C6	C7	C8	C9	C10	C11	C12	C13
Taxonomic Order richness	-0.35	-0.22	0.03	0.00	-0.20	-0.16	0.60	0.60	-0.16	0.11	-0.02	-0.00	-0.35
Mean annual temperature	-0.19	-0.46	-0.02	-0.2	-0.05	0.04	-0.22	-0.00	0.11	-0.14	0.05	0.79	-0.19
Mean temperature of the coldest quarter	-0.22	-0.43	0.03	-0.24	-0.11	0.07	-0.19	0.02	0.14	-0.57	0.02	-0.55	-0.22
Mean temperature of the warmest quarter	-0.11	-0.47	-0.12	-0.08	0.08	0.02	-0.27	-0.07	0.06	0.77	-0.05	-0.26	-0.11
Mean annual precipitations	-0.45	0.15	0.03	-0.10	-0.05	0.29	0.12	-0.33	-0.11	0.01	-0.74	0.03	-0.45
Precipitations of the wettest quarter	-0.45	0.11	0.05	-0.08	-0.08	0.21	0.23	-0.45	-0.14	0.09	0.66	-0.03	-0.45
Precipitations of the driest quarter	-0.25	0.32	0.08	-0.05	0.16	0.52	-0.43	0.56	-0.12	0.05	0.12	-0.00	-0.25
Time since last glacial retreat	-0.10	-0.3	0.26	0.46	0.75	0.05	0.13	-0.06	-0.16	-0.14	-0.01	0.00	-0.10
Elevation range	-0.05	0.06	0.92	-0.02	-0.20	-0.21	-0.14	-0.02	0.17	0.13	-0.02	-0.00	-0.05
Primary productivity	-0.35	0.24	-0.16	0.01	0.28	-0.21	0.09	0.06	0.81	0.03	0.02	0.00	-0.35
Primary productivity seasonality	-0.32	0.20	-0.11	-0.23	0.21	-0.69	-0.31	-0.01	-0.42	-0.05	-0.00	-0.01	-0.32
Actual evapotranspiration	-0.27	-0.02	-0.15	0.79	-0.43	-0.11	-0.30	-0.03	0.00	-0.05	-0.00	-0.00	-0.27

Table S4. Moran Index test results for OLS model's residuals. The Moran Index test the null hypothesis of no spatial autocorrelation. C1-2 = First two principal components explaining ~ 65% of the variance of environmental variables and order richness; Acc = Accessibility; pAg = Percentage of agricultural areas; PD = Population density; YFU = Year from first land use; ISL = factor to classify cells as islands (ISL1 = <25,000 km²; ISL2= <100,000 km²; ISL3 = <500,000 km²; ISL4 = <750,000,000 km²).

Model	Observed	Expectation	Variance	p-value
<i>Med ~ C1+C2</i>	0.9241	-0.0002	3.7465×10 ⁻⁵	< 2.2×10 ⁻¹⁶
<i>Med ~ C1+C2+Acc</i>	0.9031	-0.0003	3.7461×10 ⁻⁵	< 2.2×10 ⁻¹⁶
<i>Med ~ C1+C2+pAg</i>	0.9179	-0.0003	3.7462×10 ⁻⁵	< 2.2×10 ⁻¹⁶
<i>Med ~ C1+C2+PD</i>	0.9068	-0.0003	3.7461×10 ⁻⁵	< 2.2×10 ⁻¹⁶
<i>Med ~ C1+C2+Acc+pAg</i>	0.9026	-0.0003	3.7458×10 ⁻⁵	< 2.2×10 ⁻¹⁶
<i>Med ~ C1+C2+YFU</i>	0.9162	-0.0003	3.7461×10 ⁻⁵	< 2.2×10 ⁻¹⁶
<i>Med ~ C1+C2+YFU+PD</i>	0.908	-0.0003	3.7457×10 ⁻⁵	< 2.2×10 ⁻¹⁶
<i>Med ~ C1+C2+YFU+Acc</i>	0.9014	-0.0003	3.7458×10 ⁻⁵	< 2.2×10 ⁻¹⁶
<i>Med ~ ISL1+C1+C2</i>	0.9241	-0.0002	3.7463×10 ⁻⁵	< 2.2×10 ⁻¹⁶
<i>Med ~ ISL1+C1+C2+Acc</i>	0.9031	-0.0003	3.7459×10 ⁻⁵	< 2.2×10 ⁻¹⁶
<i>Med ~ ISL1+C1+C2+pAg</i>	0.918	-0.0003	3.7459×10 ⁻⁵	< 2.2×10 ⁻¹⁶
<i>Med ~ ISL1+C1+C2+PD</i>	0.9068	-0.0003	3.7459×10 ⁻⁵	< 2.2×10 ⁻¹⁶
<i>Med ~ ISL1+C1+C2+Acc+pAg</i>	0.9025	-0.0003	3.7455×10 ⁻⁵	< 2.2×10 ⁻¹⁶
<i>Med ~ ISL1+C1+C2+YFU</i>	0.9162	-0.0003	3.7459×10 ⁻⁵	< 2.2×10 ⁻¹⁶
<i>Med ~ ISL1+C1+C2+YFU+PD</i>	0.9081	-0.0003	3.7455×10 ⁻⁵	< 2.2×10 ⁻¹⁶
<i>Med ~ ISL1+C1+C2+YFU+Acc</i>	0.9014	-0.0003	3.7455×10 ⁻⁵	< 2.2×10 ⁻¹⁶
<i>Med ~ ISL2+C1+C2</i>	0.9241	-0.0002	3.7461×10 ⁻⁵	< 2.2×10 ⁻¹⁶
<i>Med ~ ISL2+C1+C2+Acc</i>	0.903	-0.0003	3.7457×10 ⁻⁵	< 2.2×10 ⁻¹⁶
<i>Med ~ ISL2+C1+C2+pAg</i>	0.9178	-0.0003	3.7457×10 ⁻⁵	< 2.2×10 ⁻¹⁶
<i>Med ~ ISL2+C1+C2+PD</i>	0.9066	-0.0003	3.7456×10 ⁻⁵	< 2.2×10 ⁻¹⁶
<i>Med ~ ISL2+C1+C2+Acc+pAg</i>	0.9025	-0.0004	3.7453×10 ⁻⁵	< 2.2×10 ⁻¹⁶

Model	Observed	Expectation	Variance	p-value
<i>Med ~ ISL2+C1+C2+YFU</i>	0.916	-0.0003	3.7457×10^{-5}	$< 2.2 \times 10^{-16}$
<i>Med ~ ISL2+C1+C2+YFU+PD</i>	0.9079	-0.0004	3.7453×10^{-5}	$< 2.2 \times 10^{-16}$
<i>Med ~ ISL2+C1+C2+YFU+Acc</i>	0.9014	-0.0004	3.7453×10^{-5}	$< 2.2 \times 10^{-16}$
<i>Med ~ ISL3+C1+C2</i>	0.9241	-0.0003	3.7460×10^{-5}	$< 2.2 \times 10^{-16}$
<i>Med ~ ISL3+C1+C2+Acc</i>	0.9031	-0.0003	3.7456×10^{-5}	$< 2.2 \times 10^{-16}$
<i>Med ~ ISL3+C1+C2+pAg</i>	0.918	-0.0003	3.7457×10^{-5}	$< 2.2 \times 10^{-16}$
<i>Med ~ ISL3+C1+C2+PD</i>	0.9067	-0.0003	3.7456×10^{-5}	$< 2.2 \times 10^{-16}$
<i>Med ~ ISL3+C1+C2+Acc+pAg</i>	0.9025	-0.0004	3.7453×10^{-5}	$< 2.2 \times 10^{-16}$
<i>Med ~ ISL3+C1+C2+YFU</i>	0.9162	-0.0003	3.7456×10^{-5}	$< 2.2 \times 10^{-16}$
<i>Med ~ ISL3+C1+C2+YFU+PD</i>	0.908	-0.0004	3.7452×10^{-5}	$< 2.2 \times 10^{-16}$
<i>Med ~ ISL3+C1+C2+YFU+Acc</i>	0.9014	-0.0004	3.7453×10^{-5}	$< 2.2 \times 10^{-16}$
<i>Med ~ ISL4+C1+C2</i>	0.9214	-0.0003	3.7461×10^{-5}	$< 2.2 \times 10^{-16}$
<i>Med ~ ISL4+C1+C2+Acc</i>	0.9012	-0.0003	3.7457×10^{-5}	$< 2.2 \times 10^{-16}$
<i>Med ~ ISL4+C1+C2+pAg</i>	0.9135	-0.0003	3.7457×10^{-5}	$< 2.2 \times 10^{-16}$
<i>Med ~ ISL4+C1+C2+PD</i>	0.9033	-0.0003	3.7456×10^{-5}	$< 2.2 \times 10^{-16}$
<i>Med ~ ISL4+C1+C2+Acc+pAg</i>	0.9013	-0.0004	3.7453×10^{-5}	$< 2.2 \times 10^{-16}$
<i>Med ~ ISL4+C1+C2+YFU</i>	0.9127	-0.0003	3.7457×10^{-5}	$< 2.2 \times 10^{-16}$
<i>Med ~ ISL4+C1+C2+YFU+PD</i>	0.9046	-0.0004	3.7453×10^{-5}	$< 2.2 \times 10^{-16}$
<i>Med ~ ISL4+C1+C2+YFU+Acc</i>	0.9002	-0.0004	3.7453×10^{-5}	$< 2.2 \times 10^{-16}$
<i>Max ~ C1+C2</i>	0.8983	-0.0002	3.8086×10^{-5}	$< 2.2 \times 10^{-16}$
<i>Max ~ C1+C2+Acc</i>	0.8789	-0.0003	3.8082×10^{-5}	$< 2.2 \times 10^{-16}$
<i>Max ~ C1+C2+pAg</i>	0.8818	-0.0003	3.8082×10^{-5}	$< 2.2 \times 10^{-16}$
<i>Max ~ C1+C2+PD</i>	0.8855	-0.0003	3.8082×10^{-5}	$< 2.2 \times 10^{-16}$
<i>Max ~ C1+C2+Acc+pAg</i>	0.8779	-0.0003	3.8078×10^{-5}	$< 2.2 \times 10^{-16}$
<i>Max ~ C1+C2+YFU</i>	0.89	-0.0003	3.8082×10^{-5}	$< 2.2 \times 10^{-16}$
<i>Max ~ C1+C2+YFU+PD</i>	0.8862	-0.0003	3.8078×10^{-5}	$< 2.2 \times 10^{-16}$

Model	Observed	Expectation	Variance	p-value
<i>Max ~ C1+C2+YFU+Acc</i>	0.8782	-0.0003	3.8078×10^{-5}	$< 2.2 \times 10^{-16}$
<i>Max ~ ISL1+C1+C2</i>	0.8987	-0.0002	3.8083×10^{-5}	$< 2.2 \times 10^{-16}$
<i>Max ~ ISL1+C1+C2+Acc</i>	0.8791	-0.0003	3.8079×10^{-5}	$< 2.2 \times 10^{-16}$
<i>Max ~ ISL1+C1+C2+pAg</i>	0.8825	-0.0003	3.8079×10^{-5}	$< 2.2 \times 10^{-16}$
<i>Max ~ ISL1+C1+C2+PD</i>	0.8861	-0.0003	3.8079×10^{-5}	$< 2.2 \times 10^{-16}$
<i>Max ~ ISL1+C1+C2+Acc+pAg</i>	0.8783	-0.0004	3.8075×10^{-5}	$< 2.2 \times 10^{-16}$
<i>Max ~ ISL1+C1+C2+YFU</i>	0.8907	-0.0003	3.8079×10^{-5}	$< 2.2 \times 10^{-16}$
<i>Max ~ ISL1+C1+C2+YFU+PD</i>	0.8868	-0.0003	3.8075×10^{-5}	$< 2.2 \times 10^{-16}$
<i>Max ~ ISL1+C1+C2+YFU+Acc</i>	0.8781	-0.0003	3.8075×10^{-5}	$< 2.2 \times 10^{-16}$
<i>Max ~ ISL2+C1+C2</i>	0.8987	-0.0003	3.8081×10^{-5}	$< 2.2 \times 10^{-16}$
<i>Max ~ ISL2+C1+C2+Acc</i>	0.8799	-0.0003	3.8077×10^{-5}	$< 2.2 \times 10^{-16}$
<i>Max ~ ISL2+C1+C2+pAg</i>	0.8826	-0.0003	3.8077×10^{-5}	$< 2.2 \times 10^{-16}$
<i>Max ~ ISL2+C1+C2+PD</i>	0.8865	-0.0003	3.8077×10^{-5}	$< 2.2 \times 10^{-16}$
<i>Max ~ ISL2+C1+C2+Acc+pAg</i>	0.8788	-0.0004	3.8073×10^{-5}	$< 2.2 \times 10^{-16}$
<i>Max ~ ISL2+C1+C2+YFU</i>	0.891	-0.0003	3.8077×10^{-5}	$< 2.2 \times 10^{-16}$
<i>Max ~ ISL2+C1+C2+YFU+PD</i>	0.8872	-0.0004	3.8073×10^{-5}	$< 2.2 \times 10^{-16}$
<i>Max ~ ISL2+C1+C2+YFU+Acc</i>	0.8788	-0.0004	3.8073×10^{-5}	$< 2.2 \times 10^{-16}$
<i>Max ~ ISL3+C1+C2</i>	0.8993	-0.0003	3.8081×10^{-5}	$< 2.2 \times 10^{-16}$
<i>Max ~ ISL3+C1+C2+Acc</i>	0.881	-0.0003	3.8077×10^{-5}	$< 2.2 \times 10^{-16}$
<i>Max ~ ISL3+C1+C2+pAg</i>	0.8834	-0.0003	3.8077×10^{-5}	$< 2.2 \times 10^{-16}$
<i>Max ~ ISL3+C1+C2+PD</i>	0.8875	-0.0003	3.8077×10^{-5}	$< 2.2 \times 10^{-16}$
<i>Max ~ ISL3+C1+C2+Acc+pAg</i>	0.8797	-0.0004	3.8073×10^{-5}	$< 2.2 \times 10^{-16}$
<i>Max ~ ISL3+C1+C2+YFU</i>	0.8917	-0.0003	3.8077×10^{-5}	$< 2.2 \times 10^{-16}$
<i>Max ~ ISL3+C1+C2+YFU+PD</i>	0.8881	-0.0004	3.8073×10^{-5}	$< 2.2 \times 10^{-16}$
<i>Max ~ ISL3+C1+C2+YFU+Acc</i>	0.88	-0.0004	3.8073×10^{-5}	$< 2.2 \times 10^{-16}$
<i>Max ~ ISL4+C1+C2</i>	0.8967	-0.0003	3.8081×10^{-5}	$< 2.2 \times 10^{-16}$
<i>Max ~ ISL4+C1+C2+Acc</i>	0.8759	-0.0003	3.8077×10^{-5}	$< 2.2 \times 10^{-16}$

Model	Observed	Expectation	Variance	p-value
<i>Max ~ ISL4+C1+C2+pAg</i>	0.8816	-0.0003	3.8077×10^{-5}	$< 2.2 \times 10^{-16}$
<i>Max ~ ISL4+C1+C2+PD</i>	0.8849	-0.0003	3.8077×10^{-5}	$< 2.2 \times 10^{-16}$
<i>Max ~ ISL4+C1+C2+Acc+pAg</i>	0.8757	-0.0004	3.8073×10^{-5}	$< 2.2 \times 10^{-16}$
<i>Max ~ ISL4+C1+C2+YFU</i>	0.8887	-0.0003	3.8077×10^{-5}	$< 2.2 \times 10^{-16}$
<i>Max ~ ISL4+C1+C2+YFU+PD</i>	0.8854	-0.0004	3.8073×10^{-5}	$< 2.2 \times 10^{-16}$
<i>Max ~ ISL4+C1+C2+YFU+Acc</i>	0.8742	-0.0004	3.8073×10^{-5}	$< 2.2 \times 10^{-16}$
<i>Skew ~ C1+C2</i>	0.81	-0.0002	3.7465×10^{-5}	$< 2.2 \times 10^{-16}$
<i>Skew ~ C1+C2+Acc</i>	0.7862	-0.0003	3.7461×10^{-5}	$< 2.2 \times 10^{-16}$
<i>Skew ~ C1+C2+pAg</i>	0.7988	-0.0003	3.7462×10^{-5}	$< 2.2 \times 10^{-16}$
<i>Skew ~ C1+C2+PD</i>	0.7881	-0.0003	3.7461×10^{-5}	$< 2.2 \times 10^{-16}$
<i>Skew ~ C1+C2+Acc+pAg</i>	0.7875	-0.0003	3.7458×10^{-5}	$< 2.2 \times 10^{-16}$
<i>Skew ~ C1+C2+YFU</i>	0.7916	-0.0003	3.7461×10^{-5}	$< 2.2 \times 10^{-16}$
<i>Skew ~ C1+C2+YFU+PD</i>	0.7867	-0.0003	3.7457×10^{-5}	$< 2.2 \times 10^{-16}$
<i>Skew ~ C1+C2+YFU+Acc</i>	0.7865	-0.0003	3.7458×10^{-5}	$< 2.2 \times 10^{-16}$
<i>Skew ~ ISL1+C1+C2</i>	0.8086	-0.0002	3.7463×10^{-5}	$< 2.2 \times 10^{-16}$
<i>Skew ~ ISL1+C1+C2+Acc</i>	0.7842	-0.0003	3.7459×10^{-5}	$< 2.2 \times 10^{-16}$
<i>Skew ~ ISL1+C1+C2+pAg</i>	0.7979	-0.0003	3.7459×10^{-5}	$< 2.2 \times 10^{-16}$
<i>Skew ~ ISL1+C1+C2+PD</i>	0.7866	-0.0003	3.7459×10^{-5}	$< 2.2 \times 10^{-16}$
<i>Skew ~ ISL1+C1+C2+Acc+pAg</i>	0.7858	-0.0003	3.7455×10^{-5}	$< 2.2 \times 10^{-16}$
<i>Skew ~ ISL1+C1+C2+YFU</i>	0.7905	-0.0003	3.7459×10^{-5}	$< 2.2 \times 10^{-16}$
<i>Skew ~ ISL1+C1+C2+YFU+PD</i>	0.7854	-0.0003	3.7455×10^{-5}	$< 2.2 \times 10^{-16}$
<i>Skew ~ ISL1+C1+C2+YFU+Acc</i>	0.7849	-0.0003	3.7455×10^{-5}	$< 2.2 \times 10^{-16}$
<i>Skew ~ ISL2+C1+C2</i>	0.8098	-0.0002	3.7461×10^{-5}	$< 2.2 \times 10^{-16}$
<i>Skew ~ ISL2+C1+C2+Acc</i>	0.7861	-0.0003	3.7457×10^{-5}	$< 2.2 \times 10^{-16}$
<i>Skew ~ ISL2+C1+C2+pAg</i>	0.7987	-0.0003	3.7457×10^{-5}	$< 2.2 \times 10^{-16}$
<i>Skew ~ ISL2+C1+C2+PD</i>	0.788	-0.0003	3.7456×10^{-5}	$< 2.2 \times 10^{-16}$

Model	Observed	Expectation	Variance	p-value
<i>Skew ~ ISL2+C1+C2+Acc+pAg</i>	0.7874	-0.0004	3.7453×10^{-5}	$< 2.2 \times 10^{-16}$
<i>Skew ~ ISL2+C1+C2+YFU</i>	0.7916	-0.0003	3.7457×10^{-5}	$< 2.2 \times 10^{-16}$
<i>Skew ~ ISL2+C1+C2+YFU+PD</i>	0.7867	-0.0004	3.7453×10^{-5}	$< 2.2 \times 10^{-16}$
<i>Skew ~ ISL2+C1+C2+YFU+Acc</i>	0.7865	-0.0004	3.7453×10^{-5}	$< 2.2 \times 10^{-16}$
<i>Skew ~ ISL3+C1+C2</i>	0.8079	-0.0003	3.7460×10^{-5}	$< 2.2 \times 10^{-16}$
<i>Skew ~ ISL3+C1+C2+Acc</i>	0.7849	-0.0003	3.7456×10^{-5}	$< 2.2 \times 10^{-16}$
<i>Skew ~ ISL3+C1+C2+pAg</i>	0.7977	-0.0003	3.7457×10^{-5}	$< 2.2 \times 10^{-16}$
<i>Skew ~ ISL3+C1+C2+PD</i>	0.787	-0.0003	3.7456×10^{-5}	$< 2.2 \times 10^{-16}$
<i>Skew ~ ISL3+C1+C2+Acc+pAg</i>	0.7862	-0.0004	3.7453×10^{-5}	$< 2.2 \times 10^{-16}$
<i>Skew ~ ISL3+C1+C2+YFU</i>	0.7905	-0.0003	3.7456×10^{-5}	$< 2.2 \times 10^{-16}$
<i>Skew ~ ISL3+C1+C2+YFU+PD</i>	0.7857	-0.0004	3.7452×10^{-5}	$< 2.2 \times 10^{-16}$
<i>Skew ~ ISL3+C1+C2+YFU+Acc</i>	0.7854	-0.0004	3.7453×10^{-5}	$< 2.2 \times 10^{-16}$
<i>Skew ~ ISL4+C1+C2</i>	0.8085	-0.0003	3.7461×10^{-5}	$< 2.2 \times 10^{-16}$
<i>Skew ~ ISL4+C1+C2+Acc</i>	0.7829	-0.0003	3.7457×10^{-5}	$< 2.2 \times 10^{-16}$
<i>Skew ~ ISL4+C1+C2+pAg</i>	0.7982	-0.0003	3.7457×10^{-5}	$< 2.2 \times 10^{-16}$
<i>Skew ~ ISL4+C1+C2+PD</i>	0.7863	-0.0003	3.7456×10^{-5}	$< 2.2 \times 10^{-16}$
<i>Skew ~ ISL4+C1+C2+Acc+pAg</i>	0.7846	-0.0004	3.7453×10^{-5}	$< 2.2 \times 10^{-16}$
<i>Skew ~ ISL4+C1+C2+YFU</i>	0.7903	-0.0003	3.7457×10^{-5}	$< 2.2 \times 10^{-16}$
<i>Skew ~ ISL4+C1+C2+YFU+PD</i>	0.7851	-0.0004	3.7453×10^{-5}	$< 2.2 \times 10^{-16}$
<i>Skew ~ ISL4+C1+C2+YFU+Acc</i>	0.7837	-0.0004	3.7453×10^{-5}	$< 2.2 \times 10^{-16}$

Table S5. Comparison of models explaining the observed distribution of median (Med), maximum body mass (Max) and body mass skewness (Skew). df = degree of freedom; BIC = Bayesian Information Criterion; Δ BIC = difference in BIC with the best model; ω = BIC weight; R^2_{sp} = variance explained by the fixed factor and the spatial autocorrelation combined; R^2_{nsp} = variance explained by the fixed factors only. C1-2 = First two principal components explaining ~ 65% of the variance of environmental variables and order richness; Acc = Accessibility; pAg = Percentage of agricultural areas; PD = Population density; YFU = Year from first land use; ISL = factor to classify cells as islands (ISL1 = <25,000 km²; ISL2= <100,000 km²; ISL3 = <500,000 km²; ISL4 = <750,000,000 km²).

Model	df	BIC	Δ BIC	ω	R^2_{sp}	R^2_{nsp}
<i>Med ~ C1 + C2 + YFU + Acc</i>	7	-8564.032	0	0.952	0.941	0.082
<i>Med ~ ISL4 + C1 + C2 + YFU + Acc</i>	8	-8557.369	6.662	0.034	0.941	0.086
<i>Med ~ ISL2 + C1 + C2 + YFU + Acc</i>	8	-8555.244	8.787	0.012	0.941	0.083
<i>Med ~ C1 + C2 + Acc</i>	6	-8550.977	13.054	0.001	0.941	0.091
<i>Med ~ C1 + C2 + Acc + pAg</i>	7	-8546.472	17.560	0	0.941	0.086
<i>Med ~ C1 + C2 + YFU + PD</i>	7	-8545.785	18.247	0	0.941	0.062
<i>Med ~ ISL4 + C1 + C2 + Acc</i>	7	-8544.118	19.914	0	0.941	0.096
<i>Med ~ ISL2 + C1 + C2 + Acc</i>	7	-8542.136	21.895	0	0.941	0.093
<i>Med ~ ISL4 + C1 + C2 + Acc + pAg</i>	8	-8540.032	24.000	0	0.941	0.091
<i>Med ~ ISL4 + C1 + C2 + YFU + PD</i>	8	-8539.507	24.525	0	0.941	0.067
<i>Med ~ ISL2 + C1 + C2 + Acc + pAg</i>	8	-8537.844	26.187	0	0.941	0.087
<i>Med ~ ISL2 + C1 + C2 + YFU + PD</i>	8	-8537.146	26.886	0	0.941	0.063
<i>Med ~ C1 + C2 + YFU</i>	6	-8532.794	31.238	0	0.941	0.046
<i>Med ~ C1 + C2 + PD</i>	6	-8527.818	36.213	0	0.941	0.068
<i>Med ~ ISL4 + C1 + C2 + YFU</i>	7	-8526.811	37.221	0	0.941	0.05
<i>Med ~ ISL2 + C1 + C2 + YFU</i>	7	-8524.359	39.672	0	0.941	0.047
<i>Med ~ ISL4 + C1 + C2 + PD</i>	7	-8521.359	42.673	0	0.941	0.074
<i>Med ~ ISL2 + C1 + C2 + PD</i>	7	-8519.137	44.894	0	0.941	0.069
<i>Med ~ C1 + C2 + pAg</i>	6	-8516.601	47.431	0	0.941	0.040
<i>Med ~ ISL4 + C1 + C2 + pAg</i>	7	-8511.129	52.903	0	0.941	0.045

Model	df	BIC	ΔBIC	ω	R²_{sp}	R²_{nsp}
<i>Med ~ C1 + C2</i>	5	-8509.927	54.104	0	0.94	0.045
<i>Med ~ ISL2 + C1 + C2 + pAg</i>	7	-8508.521	55.511	0	0.941	0.041
<i>Med ~ ISL4 + C1 + C2</i>	6	-8503.772	60.259	0	0.941	0.049
<i>Med ~ ISL2 + C1 + C2</i>	6	-8501.469	62.563	0	0.941	0.045
<i>Med ~ ISL1 + C1 + C2 + YFU + Acc</i>	8	-8483.757	80.275	0	0.941	0.082
<i>Med ~ ISL1 + C1 + C2 + Acc</i>	7	-8475.722	88.309	0	0.941	0.092
<i>Med ~ ISL3 + C1 + C2 + YFU + Acc</i>	8	-8470.895	93.136	0	0.941	0.082
<i>Med ~ ISL1 + C1 + C2 + Acc + pAg</i>	8	-8467.400	96.632	0	0.941	0.086
<i>Med ~ ISL3 + C1 + C2 + Acc</i>	7	-8463.246	100.785	0	0.941	0.092
<i>Med ~ ISL1 + C1 + C2 + YFU + PD</i>	8	-8460.357	103.675	0	0.941	0.062
<i>Med ~ ISL1 + C1 + C2 + YFU</i>	7	-8456.616	107.415	0	0.941	0.046
<i>Med ~ ISL3 + C1 + C2 + Acc + pAg</i>	8	-8454.669	109.363	0	0.941	0.086
<i>Med ~ ISL3 + C1 + C2 + YFU + PD</i>	8	-8447.793	116.238	0	0.941	0.062
<i>Med ~ ISL1 + C1 + C2 + PD</i>	7	-8446.668	117.363	0	0.941	0.068
<i>Med ~ ISL3 + C1 + C2 + YFU</i>	7	-8444.437	119.594	0	0.941	0.046
<i>Med ~ ISL1 + C1 + C2</i>	6	-8439.581	124.450	0	0.941	0.045
<i>Med ~ ISL1 + C1 + C2 + pAg</i>	7	-8438.970	125.062	0	0.941	0.04
<i>Med ~ ISL3 + C1 + C2 + PD</i>	7	-8434.580	129.452	0	0.941	0.068
<i>Med ~ ISL3 + C1 + C2</i>	6	-8427.942	136.090	0	0.94	0.045
<i>Med ~ ISL3 + C1 + C2 + pAg</i>	7	-8426.588	137.444	0	0.941	0.040
<i>Max ~ ISL4 + C1 + C2 + Acc</i>	7	-17291.362	0	0.943	0.925	0.218
<i>Max ~ ISL4 + C1 + C2 + Acc + pAg</i>	8	-17285.137	6.225	0.042	0.925	0.215
<i>Max ~ ISL4 + C1 + C2 + YFU + Acc</i>	8	-17283.096	8.267	0.015	0.925	0.216
<i>Max ~ ISL2 + C1 + C2 + Acc</i>	7	-17264.127	27.236	0	0.925	0.176
<i>Max ~ ISL2 + C1 + C2 + Acc + pAg</i>	8	-17258.339	33.024	0	0.925	0.173
<i>Max ~ ISL2 + C1 + C2 + YFU + Acc</i>	8	-17256.035	35.328	0	0.925	0.173

Model	df	BIC	ΔBIC	ω	R²_{sp}	R²_{nsp}
<i>Max ~ ISL4 + C1 + C2 + PD</i>	7	-17243.395	47.968	0	0.925	0.138
<i>Max ~ ISL4 + C1 + C2 + YFU + PD</i>	8	-17237.463	53.899	0	0.925	0.141
<i>Max ~ ISL4 + C1 + C2 + pAg</i>	7	-17237.179	54.184	0	0.925	0.124
<i>Max ~ ISL4 + C1 + C2</i>	6	-17230.968	60.395	0	0.925	0.105
<i>Max ~ ISL4 + C1 + C2 + YFU</i>	7	-17226.768	64.595	0	0.925	0.113
<i>Max ~ C1 + C2 + Acc</i>	6	-17224.934	66.428	0	0.924	0.173
<i>Max ~ C1 + C2 + Acc + pAg</i>	7	-17220.831	70.532	0	0.924	0.169
<i>Max ~ ISL2 + C1 + C2 + PD</i>	7	-17217.987	73.376	0	0.924	0.099
<i>Max ~ C1 + C2 + YFU + Acc</i>	7	-17217.072	74.290	0	0.924	0.169
<i>Max ~ ISL2 + C1 + C2 + pAg</i>	7	-17212.767	78.595	0	0.924	0.086
<i>Max ~ ISL2 + C1 + C2 + YFU + PD</i>	8	-17212.269	79.094	0	0.924	0.102
<i>Max ~ ISL2 + C1 + C2</i>	6	-17206.012	85.350	0	0.924	0.065
<i>Max ~ ISL2 + C1 + C2 + YFU</i>	7	-17202.041	89.322	0	0.924	0.073
<i>Max ~ C1 + C2 + PD</i>	6	-17181.267	110.095	0	0.924	0.093
<i>Max ~ C1 + C2 + pAg</i>	6	-17179.147	112.216	0	0.924	0.083
<i>Max ~ C1 + C2 + YFU + PD</i>	7	-17175.813	115.550	0	0.924	0.097
<i>Max ~ C1 + C2</i>	5	-17169.744	121.619	0	0.924	0.061
<i>Max ~ C1 + C2 + YFU</i>	6	-17166.060	125.302	0	0.924	0.069
<i>Max ~ ISL3 + C1 + C2 + Acc</i>	7	-16968.042	323.321	0	0.925	0.172
<i>Max ~ ISL3 + C1 + C2 + Acc + pAg</i>	8	-16960.956	330.407	0	0.925	0.170
<i>Max ~ ISL3 + C1 + C2 + YFU + Acc</i>	8	-16959.704	331.658	0	0.925	0.169
<i>Max ~ ISL1 + C1 + C2 + Acc</i>	7	-16930.867	360.496	0	0.925	0.173
<i>Max ~ ISL1 + C1 + C2 + Acc + pAg</i>	8	-16924.547	366.816	0	0.925	0.171
<i>Max ~ ISL1 + C1 + C2 + YFU + Acc</i>	8	-16922.507	368.856	0	0.925	0.170
<i>Max ~ ISL3 + C1 + C2 + PD</i>	7	-16900.981	390.381	0	0.925	0.099
<i>Max ~ ISL3 + C1 + C2 + pAg</i>	7	-16896.481	394.881	0	0.925	0.087
<i>Max ~ ISL3 + C1 + C2 + YFU + PD</i>	8	-16895.813	395.550	0	0.925	0.102

Model	df	BIC	ΔBIC	ω	R^2_{sp}	R^2_{nsp}
<i>Max ~ ISL3 + C1 + C2</i>	6	-16889.228	402.134	0	0.925	0.068
<i>Max ~ ISL3 + C1 + C2 + YFU</i>	7	-16885.710	405.652	0	0.925	0.075
<i>Max ~ ISL1 + C1 + C2 + PD</i>	7	-16864.473	426.890	0	0.924	0.095
<i>Max ~ ISL1 + C1 + C2 + pAg</i>	7	-16861.819	429.544	0	0.924	0.083
<i>Max ~ ISL1 + C1 + C2 + YFU + PD</i>	8	-16859.229	432.134	0	0.924	0.098
<i>Max ~ ISL1 + C1 + C2</i>	6	-16852.920	438.442	0	0.924	0.062
<i>Max ~ ISL1 + C1 + C2 + YFU</i>	7	-16849.294	442.068	0	0.924	0.07
<i>Skew ~ ISL4 + C1 + C2 + YFU + Acc</i>	8	-39027.210	0	0.428	0.906	0.317
<i>Skew ~ ISL4 + C1 + C2 + Acc + pAg</i>	8	-39026.665	0.545	0.326	0.906	0.314
<i>Skew ~ ISL4 + C1 + C2 + Acc</i>	7	-39025.271	1.939	0.162	0.906	0.314
<i>Skew ~ ISL2 + C1 + C2 + YFU + Acc</i>	8	-39022.476	4.734	0.04	0.906	0.311
<i>Skew ~ ISL2 + C1 + C2 + Acc + pAg</i>	8	-39021.693	5.517	0.027	0.906	0.307
<i>Skew ~ ISL2 + C1 + C2 + Acc</i>	7	-39020.751	6.460	0.017	0.906	0.308
<i>Skew ~ ISL4 + C1 + C2 + YFU + PD</i>	8	-39003.944	23.266	0	0.906	0.309
<i>Skew ~ ISL4 + C1 + C2 + pAg</i>	7	-39002.62	24.590	0	0.906	0.303
<i>Skew ~ ISL2 + C1 + C2 + YFU + PD</i>	8	-38998.217	28.993	0	0.906	0.301
<i>Skew ~ ISL4 + C1 + C2 + PD</i>	7	-38997.566	29.644	0	0.906	0.304
<i>Skew ~ ISL2 + C1 + C2 + pAg</i>	7	-38996.541	30.670	0	0.906	0.294
<i>Skew ~ ISL4 + C1 + C2 + YFU</i>	7	-38995.982	31.228	0	0.906	0.305
<i>Skew ~ C1 + C2 + YFU + Acc</i>	7	-38995.865	31.345	0	0.905	0.282
<i>Skew ~ C1 + C2 + Acc</i>	6	-38994.575	32.635	0	0.905	0.28
<i>Skew ~ C1 + C2 + Acc + pAg</i>	7	-38993.117	34.093	0	0.905	0.279
<i>Skew ~ ISL2 + C1 + C2 + PD</i>	7	-38992.041	35.169	0	0.906	0.296
<i>Skew ~ ISL2 + C1 + C2 + YFU</i>	7	-38990.203	37.007	0	0.906	0.297
<i>Skew ~ ISL4 + C1 + C2</i>	6	-38985.954	41.256	0	0.906	0.298
<i>Skew ~ ISL2 + C1 + C2</i>	6	-38980.429	46.781	0	0.906	0.29

Model	df	BIC	ΔBIC	ω	R²_{sp}	R²_{nsp}
<i>Skew ~ C1 + C2 + YFU + PD</i>	7	-38971.029	56.181	0	0.906	0.273
<i>Skew ~ C1 + C2 + PD</i>	6	-38965.287	61.923	0	0.906	0.269
<i>Skew ~ C1 + C2 + pAg</i>	6	-38965.246	61.964	0	0.906	0.267
<i>Skew ~ C1 + C2 + YFU</i>	6	-38961.953	65.257	0	0.906	0.270
<i>Skew ~ C1 + C2</i>	5	-38952.542	74.668	0	0.906	0.265
<i>Skew ~ ISL3 + C1 + C2</i>	6	-37803.795	1223.415	0	0.906	0.284
<i>Skew ~ ISL3 + C1 + C2 + Acc</i>	7	-37800.997	1226.213	0	0.906	0.303
<i>Skew ~ ISL3 + C1 + C2 + pAg</i>	7	-37799.445	1227.765	0	0.906	0.288
<i>Skew ~ ISL3 + C1 + C2 + YFU</i>	7	-37798.878	1228.332	0	0.906	0.291
<i>Skew ~ ISL3 + C1 + C2 + PD</i>	7	-37796.019	1231.191	0	0.906	0.29
<i>Skew ~ ISL3 + C1 + C2 + YFU + Acc</i>	8	-37794.495	1232.715	0	0.906	0.305
<i>Skew ~ ISL3 + C1 + C2 + Acc + pAg</i>	8	-37793.919	1233.291	0	0.906	0.301
<i>Skew ~ ISL1 + C1 + C2</i>	6	-37790.854	1236.356	0	0.906	0.279
<i>Skew ~ ISL3 + C1 + C2 + YFU + PD</i>	8	-37790.581	1236.629	0	0.906	0.295
<i>Skew ~ ISL1 + C1 + C2 + Acc</i>	7	-37787.999	1239.211	0	0.906	0.297
<i>Skew ~ ISL1 + C1 + C2 + YFU</i>	7	-37785.861	1241.349	0	0.906	0.286
<i>Skew ~ ISL1 + C1 + C2 + pAg</i>	7	-37785.581	1241.629	0	0.906	0.283
<i>Skew ~ ISL1 + C1 + C2 + PD</i>	7	-37783.385	1243.825	0	0.906	0.285
<i>Skew ~ ISL1 + C1 + C2 + YFU + Acc</i>	8	-37781.445	1245.765	0	0.906	0.299
<i>Skew ~ ISL1 + C1 + C2 + Acc + pAg</i>	8	-37780.278	1246.932	0	0.906	0.296
<i>Skew ~ ISL1 + C1 + C2 + YFU + PD</i>	8	-37777.834	1249.376	0	0.906	0.290

Table S6. Coefficient estimates (SE) for all models. C1-2 = First two principal components explaining ~ 65% of the variance of environmental variables and order richness; Acc = Accessibility; pAg = Percentage of agricultural areas; PD = Population density; YFU = Year from first land use; ISL = factor to classify cells as islands (ISL1 = <25,000 km²; ISL2= <100,000 km²; ISL3 = <500,000 km²; ISL4 = <750,000,000 km²). P-values: * = <0.05; ** = <0.01; *** = <0.001.

Model	Int	Comp1	Comp2	Acc	pAg	PD	YFU	ISL1	ISL2	ISL3	ISL4
<i>Med ~ C1 + C2</i>	-0.364 (0.019) ***	0.015 (0.007) *	-0.054 (0.011) ***	-	-	-	-	-	-	-	-
<i>Med ~ C1 + C2 + Acc</i>	-0.356 (0.018) ***	0.013 (0.007)	-0.071 (0.011) ***	0.035 (0.005) ***	-	-	-	-	-	-	-
<i>Med ~ C1 + C2 + pAg</i>	-0.359 (0.019) ***	0.013 (0.007)	-0.057 (0.011) ***	-	-0.014 (0.005) **	-	-	-	-	-	-
<i>Med ~ C1 + C2 + PD</i>	-0.361 (0.019) ***	0.010 (0.007)	-0.061 (0.011) ***	-	-	-0.020 (0.005) ***	-	-	-	-	-
<i>Med ~ C1 + C2 + Acc + pAg</i>	-0.354 (0.019) ***	0.012 (0.007)	-0.071 (0.011) ***	0.034 (0.005) ***	-0.005 (0.005)	-	-	-	-	-	-
<i>Med ~ C1 + C2 + YFU</i>	-0.361 (0.019) ***	0.013 (0.007)	-0.056 (0.011) ***	-	-	-	-0.020 (0.004) ***	-	-	-	-
<i>Med ~ C1 + C2 + YFU + PD</i>	-0.358 (0.019) ***	0.008 (0.007)	-0.062 (0.011) ***	-	-	-0.018 (0.005) ***	-0.019 (0.004) ***	-	-	-	-
<i>Med ~ C1 + C2 + YFU + Acc</i>	-0.354 (0.019) ***	0.011 (0.007)	-0.071 (0.011) ***	0.032 (0.005) ***	-	-	-0.017 (0.004) ***	-	-	-	-

Model	Int	Comp1	Comp2	Acc	pAg	PD	YFU	ISL1	ISL2	ISL3	ISL4
<i>Med ~ ISL1 + C1 + C2</i>	-0.385 (0.020) ***	0.015 (0.007) *	-0.054 (0.011) ***	-	-	-	-	0.065 (0.019) ***	-	-	-
<i>Med ~ ISL1 + C1 + C2 + Acc</i>	-0.377 (0.019) ***	0.012 (0.007)	-0.072 (0.011) ***	0.035 (0.005) ***	-	-	-	0.067 (0.019) ***	-	-	-
<i>Med ~ ISL1 + C1 + C2 + pAg</i>	-0.381 (0.020) ***	0.012 (0.007)	-0.057 (0.011) ***	-	-0.015 (0.005) **	-	-	0.068 (0.019) ***	-	-	-
<i>Med ~ ISL1 + C1 + C2 + PD</i>	-0.383 (0.020) ***	0.010 (0.007)	-0.061 (0.011) ***	-	-	-0.020 (0.005) ***	-	0.066 (0.019) ***	-	-	-
<i>Med ~ ISL1 + C1 + C2 + Acc + pAg</i>	-0.376 (0.020) ***	0.011 (0.007)	-0.072 (0.011) ***	0.034 (0.005) ***	-0.006 (0.005)	-	-	0.068 (0.019) ***	-	-	-
<i>Med ~ ISL1 + C1 + C2 + YFU</i>	-0.383 (0.020) ***	0.012 (0.007)	-0.056 (0.011) ***	-	-	-	-0.020 (0.004) ***	0.067 (0.019) ***	-	-	-
<i>Med ~ ISL1 + C1 + C2 + YFU + PD</i>	-0.381 (0.020) ***	0.008 (0.007)	-0.062 (0.011) ***	-	-	-0.018 (0.005) ***	-0.019 (0.004) ***	0.067 (0.019) ***	-	-	-
<i>Med ~ ISL1 + C1 + C2 + YFU + Acc</i>	-0.376 (0.019) ***	0.010 (0.007)	-0.072 (0.011) ***	0.032 (0.005) ***	-	-	-0.017 (0.004) ***	0.068 (0.019) ***	-	-	-
<i>Med ~ ISL2 + C1 + C2</i>	-0.374 (0.020) ***	0.015 (0.007) *	-0.055 (0.011) ***	-	-	-	-	-	0.026 (0.018)	-	-
<i>Med ~ ISL2 + C1 + C2 + Acc</i>	-0.366 (0.020) ***	0.012 (0.007)	-0.072 (0.011) ***	0.035 (0.005) ***	-	-	-	-	0.026 (0.018)	-	-
<i>Med ~ ISL2 + C1 + C2 + pAg</i>	-0.37 (0.020)	0.012 (0.007)	-0.057 (0.011)	-	-0.015 (0.005)	-	-	-	0.028 (0.018)	-	-

Model	Int	Comp1	Comp2	Acc	pAg	PD	YFU	ISL1	ISL2	ISL3	ISL4
	***		***		**						
<i>Med ~ ISL2 + C1 + C2 + PD</i>	-0.371 (0.020) ***	0.010 (0.007)	-0.061 (0.011) ***	-	-	-0.020 (0.005) ***	-	-	0.025 (0.018)	-	-
<i>Med ~ ISL2 + C1 + C2 + Acc + pAg</i>	-0.365 (0.020) ***	0.011 (0.007)	-0.072 (0.011) ***	0.033 (0.005) ***	-0.005 (0.005)	-	-	-	0.027 (0.018)	-	-
<i>Med ~ ISL2 + C1 + C2 + YFU</i>	-0.372 (0.020) ***	0.012 (0.007)	-0.057 (0.011) ***	-	-	-	-0.020 (0.004) ***	-	0.027 (0.018)	-	-
<i>Med ~ ISL2 + C1 + C2 + YFU + PD</i>	-0.369 (0.020) ***	0.008 (0.007)	-0.063 (0.011) ***	-	-	-0.018 (0.005) ***	-0.019 (0.004) ***	-	0.027 (0.018)	-	-
<i>Med ~ ISL2 + C1 + C2 + YFU + Acc</i>	-0.365 (0.020) ***	0.010 (0.007)	-0.072 (0.011) ***	0.032 (0.005) ***	-	-	-0.017 (0.004) ***	-	0.028 (0.018)	-	-
<i>Med ~ ISL3 + C1 + C2</i>	-0.370 (0.021) ***	0.015 (0.007) *	-0.054 (0.011) ***	-	-	-	-	-	-	0.015 (0.02)	-
<i>Med ~ ISL3 + C1 + C2 + Acc</i>	-0.362 (0.020) ***	0.013 (0.007)	-0.071 (0.011) ***	0.035 (0.005) ***	-	-	-	-	-	0.016 (0.02)	-
<i>Med ~ ISL3 + C1 + C2 + pAg</i>	-0.367 (0.021) ***	0.012 (0.007)	-0.057 (0.011) ***	-	-0.015 (0.005) **	-	-	-	-	0.018 (0.02)	-
<i>Med ~ ISL3 + C1 + C2 + PD</i>	-0.367 (0.020) ***	0.010 (0.007)	-0.061 (0.011) ***	-	-	-0.020 (0.005) ***	-	-	-	0.014 (0.02)	-
<i>Med ~ ISL3 + C1 + C2 + Acc + pAg</i>	-0.361 (0.020) ***	0.012 (0.007)	-0.072 (0.011) ***	0.034 (0.005) ***	-0.005 (0.005)	-	-	-	-	0.017 (0.02)	-

Model	Int	Comp1	Comp2	Acc	pAg	PD	YFU	ISL1	ISL2	ISL3	ISL4
<i>Med ~ ISL3 + C1 + C2 + YFU</i>	-0.367 (0.021) ***	0.012 (0.007)	-0.056 (0.011) ***	-	-	-	-0.020 (0.004) ***	-	-	0.016 (0.02)	-
<i>Med ~ ISL3 + C1 + C2 + YFU + PD</i>	-0.365 (0.020) ***	0.008 (0.007)	-0.062 (0.011) ***	-	-	-0.018 (0.005) ***	-0.019 (0.004) ***	-	-	0.015 (0.02)	-
<i>Med ~ ISL3 + C1 + C2 + YFU + Acc</i>	-0.361 (0.020) ***	0.011 (0.007)	-0.071 (0.011) ***	0.032 (0.005) ***	-	-	-0.017 (0.004) ***	-	-	0.016 (0.02)	-
<i>Med ~ ISL4 + C1 + C2</i>	-0.377 (0.021) ***	0.015 (0.007) *	-0.055 (0.011) ***	-	-	-	-	-	-	-	0.030 (0.021)
<i>Med ~ ISL4 + C1 + C2 + Acc</i>	-0.369 (0.021) ***	0.013 (0.007)	-0.072 (0.011) ***	0.035 (0.005) ***	-	-	-	-	-	-	0.031 (0.021)
<i>Med ~ ISL4 + C1 + C2 + pAg</i>	-0.374 (0.021) ***	0.012 (0.007)	-0.057 (0.011) ***	-	-0.015 (0.005) **	-	-	-	-	-	0.034 (0.021)
<i>Med ~ ISL4 + C1 + C2 + PD</i>	-0.374 (0.021) ***	0.010 (0.007)	-0.061 (0.011) ***	-	-	-0.020 (0.005) ***	-	-	-	-	0.030 (0.021)
<i>Med ~ ISL4 + C1 + C2 + Acc + pAg</i>	-0.368 (0.021) ***	0.012 (0.007)	-0.072 (0.011) ***	0.033 (0.005) ***	-0.006 (0.005)	-	-	-	-	-	0.033 (0.021)
<i>Med ~ ISL4 + C1 + C2 + YFU</i>	-0.375 (0.021) ***	0.012 (0.007)	-0.057 (0.011) ***	-	-	-	-0.020 (0.004) ***	-	-	-	0.032 (0.021)
<i>Med ~ ISL4 + C1 + C2 + YFU + PD</i>	-0.372 (0.021) ***	0.008 (0.007)	-0.062 (0.011) ***	-	-	-0.018 (0.005) ***	-0.019 (0.004) ***	-	-	-	0.032 (0.021)
<i>Med ~ ISL4 + C1 + C2 + YFU + Acc</i>	-0.368 (0.021)	0.011 (0.007)	-0.072 (0.011)	0.032 (0.005)	-	-	-0.017 (0.004)	-	-	-	0.033 (0.021)

Model	Int	Comp1	Comp2	Acc	pAg	PD	YFU	ISL1	ISL2	ISL3	ISL4
	***		***	***			***				
<i>Max ~ C1 + C2</i>	1.402 (0.014) ***	0.003 (0.005)	0.050 (0.009) ***	-	-	-	-	-	-	-	-
<i>Max ~ C1 + C2 + Acc</i>	1.415 (0.014) ***	0.001 (0.005)	0.036 (0.009) ***	0.036 (0.004) ***	-	-	-	-	-	-	-
<i>Max ~ C1 + C2 + pAg</i>	1.409 (0.014) ***	0.000 (0.006)	0.048 (0.009) ***	-	-0.017 (0.004) ***	-	-	-	-	-	-
<i>Max ~ C1 + C2 + PD</i>	1.408 (0.014) ***	-0.001 (0.006)	0.046 (0.009) ***	-	-	-0.017 (0.004) ***	-	-	-	-	-
<i>Max ~ C1 + C2 + Acc + pAg</i>	1.417 (0.014) ***	0.000 (0.005)	0.036 (0.009) ***	0.034 (0.004) ***	-0.008 (0.004) *	-	-	-	-	-	-
<i>Max ~ C1 + C2 + YFU</i>	1.404 (0.014) ***	0.002 (0.005)	0.049 (0.009) ***	-	-	-	-0.008 (0.003) *	-	-	-	-
<i>Max ~ C1 + C2 + YFU + PD</i>	1.409 (0.014) ***	-0.001 (0.006)	0.045 (0.009) ***	-	-	-0.017 (0.004) ***	-0.007 (0.003) *	-	-	-	-
<i>Max ~ C1 + C2 + YFU + Acc</i>	1.415 (0.014) ***	0.001 (0.005)	0.036 (0.009) ***	0.036 (0.004) ***	-	-	-0.004 (0.003)	-	-	-	-
<i>Max ~ ISL1 + C1 + C2</i>	1.428 (0.014) ***	0.004 (0.005)	0.050 (0.009) ***	-	-	-	-	-0.102 (0.016) ***	-	-	-
<i>Max ~ ISL1 + C1 + C2 + Acc</i>	1.438 (0.014)	0.002 (0.005)	0.037 (0.009)	0.036 (0.004)	-	-	-	-0.103 (0.016)	-	-	-

Model	Int	Comp1	Comp2	Acc	pAg	PD	YFU	ISL1	ISL2	ISL3	ISL4
	***		***	***				***			
<i>Max ~ ISL1 + C1 + C2 + pAg</i>	1.433 (0.014) ***	0.000 (0.006)	0.048 (0.009) ***	-	-0.016 (0.004) ***	-	-	-0.099 (0.016) ***	-	-	-
<i>Max ~ ISL1 + C1 + C2 + PD</i>	1.433 (0.014) ***	0.000 (0.006)	0.046 (0.009) ***	-	-	-0.017 (0.004) ***	-	-0.102 (0.016) ***	-	-	-
<i>Max ~ ISL1 + C1 + C2 + Acc + pAg</i>	1.440 (0.014) ***	0.000 (0.005)	0.036 (0.009) ***	0.034 (0.004) ***	-0.007 (0.004)	-	-	-0.101 (0.016) ***	-	-	-
<i>Max ~ ISL1 + C1 + C2 + YFU</i>	1.429 (0.014) ***	0.003 (0.005)	0.05 (0.009) ***	-	-	-	-0.007 (0.003) *	-0.101 (0.016) ***	-	-	-
<i>Max ~ ISL1 + C1 + C2 + YFU + PD</i>	1.433 (0.014) ***	-0.001 (0.006)	0.046 (0.009) ***	-	-	-0.017 (0.004) ***	-0.006 (0.003) *	-0.101 (0.016) ***	-	-	-
<i>Max ~ ISL1 + C1 + C2 + YFU + Acc</i>	1.438 (0.014) ***	0.001 (0.005)	0.037 (0.009) ***	0.036 (0.004) ***	-	-	-0.003 (0.003)	-0.102 (0.016) ***	-	-	-
<i>Max ~ ISL2 + C1 + C2</i>	1.429 (0.014) ***	0.004 (0.005)	0.050 (0.009) ***	-	-	-	-	-	-0.094 (0.015) ***	-	-
<i>Max ~ ISL2 + C1 + C2 + Acc</i>	1.439 (0.014) ***	0.002 (0.005)	0.037 (0.009) ***	0.037 (0.004) ***	-	-	-	-	-0.096 (0.015) ***	-	-
<i>Max ~ ISL2 + C1 + C2 + pAg</i>	1.433 (0.014) ***	0.001 (0.006)	0.048 (0.009) ***	-	-0.016 (0.004) ***	-	-	-	-0.092 (0.015) ***	-	-
<i>Max ~ ISL2 + C1 + C2 + PD</i>	1.434 (0.014) ***	0.000 (0.006)	0.046 (0.009) ***	-	-	-0.018 (0.004) ***	-	-	-0.095 (0.015) ***	-	-

Model	Int	Comp1	Comp2	Acc	pAg	PD	YFU	ISL1	ISL2	ISL3	ISL4
<i>Max ~ ISL2 + C1 + C2 + Acc + pAg</i>	1.440 (0.014) ***	0.000 (0.005)	0.036 (0.009) ***	0.035 (0.004) ***	-0.007 (0.004)	-	-	-	-0.095 (0.015) ***	-	-
<i>Max ~ ISL2 + C1 + C2 + YFU</i>	1.430 (0.014) ***	0.003 (0.005)	0.050 (0.009) ***	-	-	-	-0.007 (0.003) *	-	-0.094 (0.015) ***	-	-
<i>Max ~ ISL2 + C1 + C2 + YFU + PD</i>	1.434 (0.014) ***	-0.001 (0.006)	0.045 (0.009) ***	-	-	-0.017 (0.004) ***	-0.006 (0.003) *	-	-0.095 (0.015) ***	-	-
<i>Max ~ ISL2 + C1 + C2 + YFU + Acc</i>	1.439 (0.014) ***	0.001 (0.005)	0.037 (0.009) ***	0.036 (0.004) ***	-	-	-0.003 (0.003)	-	-0.096 (0.015) ***	-	-
<i>Max ~ ISL3 + C1 + C2</i>	1.445 (0.014) ***	0.003 (0.005)	0.049 (0.009) ***	-	-	-	-	-	-	-0.148 (0.017) ***	-
<i>Max ~ ISL3 + C1 + C2 + Acc</i>	1.454 (0.014) ***	0.001 (0.005)	0.035 (0.009) ***	0.037 (0.004) ***	-	-	-	-	-	-0.149 (0.017) ***	-
<i>Max ~ ISL3 + C1 + C2 + pAg</i>	1.449 (0.014) ***	0.000 (0.006)	0.047 (0.009) ***	-	-0.015 (0.004) ***	-	-	-	-	-0.144 (0.017) ***	-
<i>Max ~ ISL3 + C1 + C2 + PD</i>	1.449 (0.014) ***	-0.001 (0.006)	0.044 (0.009) ***	-	-	-0.018 (0.004) ***	-	-	-	-0.148 (0.017) ***	-
<i>Max ~ ISL3 + C1 + C2 + Acc + pAg</i>	1.455 (0.014) ***	-0.001 (0.005)	0.035 (0.009) ***	0.035 (0.004) ***	-0.006 (0.004)	-	-	-	-	-0.147 (0.017) ***	-
<i>Max ~ ISL3 + C1 + C2 + YFU</i>	1.446 (0.014) ***	0.002 (0.005)	0.048 (0.009) ***	-	-	-	-0.007 (0.003) *	-	-	-0.147 (0.017) ***	-
<i>Max ~ ISL3 + C1 + C2 + YFU + PD</i>	1.450 (0.014)	-0.002 (0.006)	0.044 (0.009)	-	-	-0.017 (0.004)	-0.006 (0.003)	-	-	-0.148 (0.017)	-

Model	Int	Comp1	Comp2	Acc	pAg	PD	YFU	ISL1	ISL2	ISL3	ISL4
	***		***			***	*			***	
<i>Max ~ ISL3 + C1 + C2 + YFU + Acc</i>	1.454 (0.014) ***	0.000 (0.005)	0.035 (0.009) ***	0.036 (0.004) ***	-	-	-0.003 (0.003)	-	-	-0.148 (0.017) ***	-
<i>Max ~ ISL4 + C1 + C2</i>	1.457 (0.014) ***	0.002 (0.005)	0.049 (0.008) ***	-	-	-	-	-	-	-	-0.181 (0.017) ***
<i>Max ~ ISL4 + C1 + C2 + Acc</i>	1.466 (0.014) ***	0.000 (0.005)	0.035 (0.009) ***	0.037 (0.004) ***	-	-	-	-	-	-	-0.183 (0.017) ***
<i>Max ~ ISL4 + C1 + C2 + pAg</i>	1.461 (0.014) ***	-0.001 (0.005)	0.047 (0.008) ***	-	-0.015 (0.004) ***	-	-	-	-	-	-0.177 (0.017) ***
<i>Max ~ ISL4 + C1 + C2 + PD</i>	1.461 (0.014) ***	-0.002 (0.006)	0.044 (0.009) ***	-	-	-0.018 (0.004) ***	-	-	-	-	-0.181 (0.017) ***
<i>Max ~ ISL4 + C1 + C2 + Acc + pAg</i>	1.467 (0.014) ***	-0.001 (0.005)	0.035 (0.009) ***	0.035 (0.004) ***	-0.006 (0.004)	-	-	-	-	-	-0.181 (0.017) ***
<i>Max ~ ISL4 + C1 + C2 + YFU</i>	1.458 (0.014) ***	0.001 (0.005)	0.049 (0.008) ***	-	-	-	-0.007 (0.003) *	-	-	-	-0.180 (0.017) ***
<i>Max ~ ISL4 + C1 + C2 + YFU + PD</i>	1.462 (0.014) ***	-0.003 (0.006)	0.044 (0.009) ***	-	-	-0.017 (0.004) ***	-0.006 (0.003) *	-	-	-	-0.181 (0.017) ***
<i>Max ~ ISL4 + C1 + C2 + YFU + Acc</i>	1.466 (0.014) ***	0.000 (0.005)	0.035 (0.009) ***	0.036 (0.004) ***	-	-	-0.003 (0.003)	-	-	-	-0.183 (0.017) ***
<i>Skew ~ C1 + C2</i>	0.536 (0.005)	-0.042 (0.002)	-0.018 (0.004)	-	-	-	-	-	-	-	-

Model	Int	Comp1	Comp2	Acc	pAg	PD	YFU	ISL1	ISL2	ISL3	ISL4
	***	***	***								
<i>Skew ~ C1 + C2 + Acc</i>	0.536 (0.005) ***	-0.042 (0.002) ***	-0.016 (0.004) ***	-0.004 (0.002) *	-	-	-	-	-	-	-
<i>Skew ~ C1 + C2 + pAg</i>	0.535 (0.005) ***	-0.041 (0.002) ***	-0.017 (0.004) ***	-	0.003 (0.002)	-	-	-	-	-	-
<i>Skew ~ C1 + C2 + PD</i>	0.536 (0.005) ***	-0.041 (0.002) ***	-0.017 (0.004) ***	-	-	0.002 (0.002)	-	-	-	-	-
<i>Skew ~ C1 + C2 + Acc + pAg</i>	0.536 (0.005) ***	-0.041 (0.002) ***	-0.016 (0.004) ***	-0.004 (0.002)	0.001 (0.002)	-	-	-	-	-	-
<i>Skew ~ C1 + C2 + YFU</i>	0.536 (0.005) ***	-0.042 (0.002) ***	-0.018 (0.004) ***	-	-	-	0.003 (0.001)	-	-	-	-
<i>Skew ~ C1 + C2 + YFU + PD</i>	0.536 (0.005) ***	-0.041 (0.002) ***	-0.017 (0.004) ***	-	-	0.002 (0.002)	0.003 (0.001)	-	-	-	-
<i>Skew ~ C1 + C2 + YFU + Acc</i>	0.536 (0.005) ***	-0.041 (0.002) ***	-0.016 (0.004) ***	-0.004 (0.002)	-	-	0.002 (0.001)	-	-	-	-
<i>Skew ~ ISL1 + C1 + C2</i>	0.550 (0.005) ***	-0.042 (0.002) ***	-0.017 (0.004) ***	-	-	-	-	-0.074 (0.007) ***	-	-	-
<i>Skew ~ ISL1 + C1 + C2 + Acc</i>	0.550 (0.005) ***	-0.042 (0.002) ***	-0.015 (0.004) ***	-0.005 (0.002) **	-	-	-	-0.075 (0.007) ***	-	-	-
<i>Skew ~ ISL1 + C1 + C2 + pAg</i>	0.550 (0.005) ***	-0.041 (0.002) ***	-0.016 (0.004) ***	-	0.004 (0.002) *	-	-	-0.075 (0.007) ***	-	-	-

Model	Int	Comp1	Comp2	Acc	pAg	PD	YFU	ISL1	ISL2	ISL3	ISL4
<i>Skew ~ ISL1 + C1 + C2 + PD</i>	0.550 (0.005) ***	-0.041 (0.002) ***	-0.016 (0.004) ***	-	-	0.003 (0.002)	-	-0.074 (0.007) ***	-	-	-
<i>Skew ~ ISL1 + C1 + C2 + Acc + pAg</i>	0.550 (0.005) ***	-0.041 (0.002) ***	-0.014 (0.004) ***	-0.004 (0.002) *	0.003 (0.002)	-	-	-0.075 (0.007) ***	-	-	-
<i>Skew ~ ISL1 + C1 + C2 + YFU</i>	0.550 (0.005) ***	-0.042 (0.002) ***	-0.016 (0.004) ***	-	-	-	0.003 (0.001) *	-0.074 (0.007) ***	-	-	-
<i>Skew ~ ISL1 + C1 + C2 + YFU + PD</i>	0.550 (0.005) ***	-0.041 (0.002) ***	-0.015 (0.004) ***	-	-	0.002 (0.002)	0.003 (0.001) *	-0.075 (0.007) ***	-	-	-
<i>Skew ~ ISL1 + C1 + C2 + YFU + Acc</i>	0.550 (0.005) ***	-0.042 (0.002) ***	-0.014 (0.004) ***	-0.004 (0.002) *	-	-	0.003 (0.001)	-0.075 (0.007) ***	-	-	-
<i>Skew ~ ISL2 + C1 + C2</i>	0.556 (0.005) ***	-0.042 (0.002) ***	-0.016 (0.004) ***	-	-	-	-	-0.085 (0.007) ***	-	-	-
<i>Skew ~ ISL2 + C1 + C2 + Acc</i>	0.556 (0.005) ***	-0.041 (0.002) ***	-0.013 (0.004) ***	-0.005 (0.002) **	-	-	-	-0.086 (0.007) ***	-	-	-
<i>Skew ~ ISL2 + C1 + C2 + pAg</i>	0.556 (0.005) ***	-0.041 (0.002) ***	-0.015 (0.004) ***	-	0.004 (0.002) *	-	-	-0.086 (0.007) ***	-	-	-
<i>Skew ~ ISL2 + C1 + C2 + PD</i>	0.556 (0.005) ***	-0.041 (0.002) ***	-0.015 (0.004) ***	-	-	0.002 (0.002)	-	-0.085 (0.007) ***	-	-	-
<i>Skew ~ ISL2 + C1 + C2 + Acc + pAg</i>	0.556 (0.005) ***	-0.041 (0.002) ***	-0.013 (0.004) ***	-0.004 (0.002) *	0.003 (0.002)	-	-	-0.086 (0.007) ***	-	-	-
<i>Skew ~ ISL2 + C1 + C2 + YFU</i>	0.556 (0.005)	-0.041 (0.002)	-0.015 (0.004)	-	-	-	0.003 (0.001)	-0.085 (0.007)	-	-	-

Model	Int	Comp1	Comp2	Acc	pAg	PD	YFU	ISL1	ISL2	ISL3	ISL4
	***	***	***				*		***		
<i>Skew ~ ISL2 + C1 + C2 + YFU + PD</i>	0.556 (0.005) ***	-0.041 (0.002) ***	-0.014 (0.004) ***	-	-	0.002 (0.002)	0.003 (0.001) *	-	-0.085 (0.007) ***	-	-
<i>Skew ~ ISL2 + C1 + C2 + YFU + Acc</i>	0.556 (0.005) ***	-0.041 (0.002) ***	-0.013 (0.004) ***	-0.004 (0.002) *	-	-	0.003 (0.001)	-	-0.086 (0.007) ***	-	-
<i>Skew ~ ISL3 + C1 + C2</i>	0.556 (0.005) ***	-0.043 (0.002) ***	-0.016 (0.004) ***	-	-	-	-	-	-	-0.081 (0.007) ***	-
<i>Skew ~ ISL3 + C1 + C2 + Acc</i>	0.557 (0.005) ***	-0.042 (0.002) ***	-0.014 (0.004) ***	-0.005 (0.002) **	-	-	-	-	-	-0.081 (0.007) ***	-
<i>Skew ~ ISL3 + C1 + C2 + pAg</i>	0.556 (0.005) ***	-0.042 (0.002) ***	-0.015 (0.004) ***	-	0.004 (0.002) *	-	-	-	-	-0.082 (0.007) ***	-
<i>Skew ~ ISL3 + C1 + C2 + PD</i>	0.557 (0.005) ***	-0.042 (0.002) ***	-0.015 (0.004) ***	-	-	0.002 (0.002)	-	-	-	-0.081 (0.007) ***	-
<i>Skew ~ ISL3 + C1 + C2 + Acc + pAg</i>	0.557 (0.005) ***	-0.042 (0.002) ***	-0.013 (0.004) ***	-0.004 (0.002) *	0.003 (0.002)	-	-	-	-	-0.082 (0.007) ***	-
<i>Skew ~ ISL3 + C1 + C2 + YFU</i>	0.557 (0.005) ***	-0.042 (0.002) ***	-0.016 (0.004) ***	-	-	-	0.003 (0.001) *	-	-	-0.081 (0.007) ***	-
<i>Skew ~ ISL3 + C1 + C2 + YFU + PD</i>	0.557 (0.005) ***	-0.042 (0.002) ***	-0.015 (0.004) ***	-	-	0.002 (0.002)	0.003 (0.001) *	-	-	-0.081 (0.007) ***	-
<i>Skew ~ ISL3 + C1 + C2 + YFU + Acc</i>	0.557 (0.005) ***	-0.042 (0.002) ***	-0.014 (0.004) ***	-0.004 (0.002) *	-	-	0.003 (0.001)	-	-	-0.081 (0.007) ***	-

Model	Int	Comp1	Comp2	Acc	pAg	PD	YFU	ISL1	ISL2	ISL3	ISL4
<i>Skew ~ ISL4 + C1 + C2</i>	0.561 (0.005) ***	-0.043 (0.002) ***	-0.015 (0.004) ***	-	-	-	-	-	-	-	-0.090 (0.007) ***
<i>Skew ~ ISL4 + C1 + C2 + Acc</i>	0.561 (0.005) ***	-0.043 (0.002) ***	-0.013 (0.004) ***	-0.005 (0.002) **	-	-	-	-	-	-	-0.090 (0.007) ***
<i>Skew ~ ISL4 + C1 + C2 + pAg</i>	0.560 (0.005) ***	-0.042 (0.002) ***	-0.014 (0.004) ***	-	0.004 (0.002) *	-	-	-	-	-	-0.091 (0.007) ***
<i>Skew ~ ISL4 + C1 + C2 + PD</i>	0.561 (0.005) ***	-0.042 (0.002) ***	-0.014 (0.004) ***	-	-	0.003 (0.002)	-	-	-	-	-0.090 (0.007) ***
<i>Skew ~ ISL4 + C1 + C2 + Acc + pAg</i>	0.561 (0.005) ***	-0.042 (0.002) ***	-0.012 (0.004) ***	-0.004 (0.002) *	0.003 (0.002)	-	-	-	-	-	-0.091 (0.007) ***
<i>Skew ~ ISL4 + C1 + C2 + YFU</i>	0.561 (0.005) ***	-0.043 (0.002) ***	-0.015 (0.004) ***	-	-	-	0.003 (0.001) *	-	-	-	-0.090 (0.007) ***
<i>Skew ~ ISL4 + C1 + C2 + YFU + PD</i>	0.561 (0.005) ***	-0.042 (0.002) ***	-0.014 (0.004) ***	-	-	0.002 (0.002)	0.003 (0.001) *	-	-	-	-0.090 (0.007) ***
<i>Skew ~ ISL4 + C1 + C2 + YFU + Acc</i>	0.561 (0.005) ***	-0.042 (0.002) ***	-0.013 (0.004) ***	-0.004 (0.002) *	-	-	0.003 (0.001)	-	-	-	-0.091 (0.007) ***

Table S5. Comparison of models explaining the observed distribution of median (Med), maximum body mass (Max) and body mass skewness (Skew). df = degree of freedom; AIC = Bayesian Information Criterion; Δ AIC = difference in AIC with the best model; ω = AIC weight; R^2_{sp} = variance explained by the fixed factor and the spatial autocorrelation combined; R^2_{nsp} = variance explained by the fixed factors only. C1-2 = First two principal components explaining ~ 65% of the variance of environmental variables and order richness; Acc = Accessibility; pAg = Percentage of agricultural areas; PD = Population density; YFU = Year from first land use; ISL = factor to classify cells as islands (ISL1 = <25,000 km²; ISL2= <100,000 km²; ISL3 = <500,000 km²; ISL4 = <750,000,000 km²).

Model	df	AIC	Δ AIC	ω	R^2_{sp}	R^2_{nsp}
<i>Med ~ ISL4 + C1 + C2 + YFU + Acc</i>	8	-8618.110	0	0.507	0.941	0.086
<i>Med ~ C1 + C2 + YFU + Acc</i>	7	-8617.18	0.930	0.318	0.941	0.082
<i>Med ~ ISL2 + C1 + C2 + YFU + Acc</i>	8	-8615.985	2.125	0.175	0.941	0.083
<i>Med ~ ISL4 + C1 + C2 + Acc + pAg</i>	8	-8600.773	17.338	0	0.941	0.091
<i>Med ~ ISL4 + C1 + C2 + YFU + PD</i>	8	-8600.248	17.862	0	0.941	0.067
<i>Med ~ C1 + C2 + Acc + pAg</i>	7	-8599.620	18.49	0	0.941	0.086
<i>Med ~ C1 + C2 + YFU + PD</i>	7	-8598.933	19.177	0	0.941	0.062
<i>Med ~ ISL2 + C1 + C2 + Acc + pAg</i>	8	-8598.585	19.525	0	0.941	0.087
<i>Med ~ ISL2 + C1 + C2 + YFU + PD</i>	8	-8597.887	20.223	0	0.941	0.063
<i>Med ~ ISL4 + C1 + C2 + Acc</i>	7	-8597.266	20.844	0	0.941	0.096
<i>Med ~ C1 + C2 + Acc</i>	6	-8596.533	21.577	0	0.941	0.091
<i>Med ~ ISL2 + C1 + C2 + Acc</i>	7	-8595.284	22.826	0	0.941	0.093
<i>Med ~ ISL4 + C1 + C2 + YFU</i>	7	-8579.959	38.151	0	0.941	0.050
<i>Med ~ C1 + C2 + YFU</i>	6	-8578.349	39.761	0	0.941	0.046
<i>Med ~ ISL2 + C1 + C2 + YFU</i>	7	-8577.507	40.603	0	0.941	0.047
<i>Med ~ ISL4 + C1 + C2 + PD</i>	7	-8574.507	43.603	0	0.941	0.074
<i>Med ~ C1 + C2 + PD</i>	6	-8573.374	44.736	0	0.941	0.068
<i>Med ~ ISL2 + C1 + C2 + PD</i>	7	-8572.285	45.825	0	0.941	0.069
<i>Med ~ ISL4 + C1 + C2 + pAg</i>	7	-8564.277	53.833	0	0.941	0.045
<i>Med ~ C1 + C2 + pAg</i>	6	-8562.156	55.954	0	0.941	0.040
<i>Med ~ ISL2 + C1 + C2 + pAg</i>	7	-8561.669	56.441	0	0.941	0.041
<i>Med ~ ISL4 + C1 + C2</i>	6	-8549.328	68.782	0	0.941	0.049

Model	df	AIC	ΔAIC	ω	R^2_{sp}	R^2_{nsp}
<i>Med ~ C1 + C2</i>	5	-8547.890	70.220	0	0.940	0.045
<i>Med ~ ISL2 + C1 + C2</i>	6	-8547.025	71.086	0	0.941	0.045
<i>Med ~ ISL1 + C1 + C2 + YFU + Acc</i>	8	-8544.498	73.612	0	0.941	0.082
<i>Med ~ ISL3 + C1 + C2 + YFU + Acc</i>	8	-8531.636	86.474	0	0.941	0.082
<i>Med ~ ISL1 + C1 + C2 + Acc</i>	7	-8528.870	89.240	0	0.941	0.092
<i>Med ~ ISL1 + C1 + C2 + Acc + pAg</i>	8	-8528.141	89.969	0	0.941	0.086
<i>Med ~ ISL1 + C1 + C2 + YFU + PD</i>	8	-8521.097	97.013	0	0.941	0.062
<i>Med ~ ISL3 + C1 + C2 + Acc</i>	7	-8516.395	101.715	0	0.941	0.092
<i>Med ~ ISL3 + C1 + C2 + Acc + pAg</i>	8	-8515.409	102.701	0	0.941	0.086
<i>Med ~ ISL1 + C1 + C2 + YFU</i>	7	-8509.765	108.345	0	0.941	0.046
<i>Med ~ ISL3 + C1 + C2 + YFU + PD</i>	8	-8508.534	109.576	0	0.941	0.062
<i>Med ~ ISL1 + C1 + C2 + PD</i>	7	-8499.817	118.294	0	0.941	0.068
<i>Med ~ ISL3 + C1 + C2 + YFU</i>	7	-8497.585	120.525	0	0.941	0.046
<i>Med ~ ISL1 + C1 + C2 + pAg</i>	7	-8492.118	125.992	0	0.941	0.040
<i>Med ~ ISL3 + C1 + C2 + PD</i>	7	-8487.728	130.382	0	0.941	0.068
<i>Med ~ ISL1 + C1 + C2</i>	6	-8485.137	132.973	0	0.941	0.045
<i>Med ~ ISL3 + C1 + C2 + pAg</i>	7	-8479.736	138.374	0	0.941	0.040
<i>Med ~ ISL3 + C1 + C2</i>	6	-8473.497	144.613	0	0.940	0.045
<i>Max ~ ISL4 + C1 + C2 + Acc + pAg</i>	8	-17345.600	0	0.534	0.925	0.215
<i>Max ~ ISL4 + C1 + C2 + Acc</i>	7	-17344.267	1.333	0.274	0.925	0.218
<i>Max ~ ISL4 + C1 + C2 + YFU + Acc</i>	8	-17343.558	2.042	0.192	0.925	0.216
<i>Max ~ ISL2 + C1 + C2 + Acc + pAg</i>	8	-17318.801	26.798	0	0.925	0.173
<i>Max ~ ISL2 + C1 + C2 + Acc</i>	7	-17317.031	28.569	0	0.925	0.176
<i>Max ~ ISL2 + C1 + C2 + YFU + Acc</i>	8	-17316.498	29.102	0	0.925	0.173
<i>Max ~ ISL4 + C1 + C2 + YFU + PD</i>	8	-17297.926	47.674	0	0.925	0.141
<i>Max ~ ISL4 + C1 + C2 + PD</i>	7	-17296.300	49.300	0	0.925	0.138
<i>Max ~ ISL4 + C1 + C2 + pAg</i>	7	-17290.083	55.517	0	0.925	0.124
<i>Max ~ ISL4 + C1 + C2</i>	7	-17279.673	65.927	0	0.925	0.113

Model	df	AIC	ΔAIC	ω	R^2_{sp}	R^2_{nsp}
+ YFU						
Max ~ ISL4 + C1 + C2	6	-17276.315	69.285	0	0.925	0.105
Max ~ C1 + C2 + Acc + pAg	7	-17273.736	71.864	0	0.924	0.169
Max ~ ISL2 + C1 + C2 + YFU + PD	8	-17272.731	72.869	0	0.924	0.102
Max ~ ISL2 + C1 + C2 + PD	7	-17270.891	74.709	0	0.924	0.099
Max ~ C1 + C2 + Acc	6	-17270.281	75.319	0	0.924	0.173
Max ~ C1 + C2 + YFU + Acc	7	-17269.977	75.623	0	0.924	0.169
Max ~ ISL2 + C1 + C2 + pAg	7	-17265.672	79.928	0	0.924	0.086
Max ~ ISL2 + C1 + C2 + YFU	7	-17254.945	90.654	0	0.924	0.073
Max ~ ISL2 + C1 + C2	6	-17251.359	94.241	0	0.924	0.065
Max ~ C1 + C2 + YFU + PD	7	-17228.718	116.882	0	0.924	0.097
Max ~ C1 + C2 + PD	6	-17226.614	118.986	0	0.924	0.093
Max ~ C1 + C2 + pAg	6	-17224.494	121.106	0	0.924	0.083
Max ~ C1 + C2 + YFU	6	-17211.407	134.193	0	0.924	0.069
Max ~ C1 + C2	5	-17207.533	138.067	0	0.924	0.061
Max ~ ISL3 + C1 + C2 + Acc + pAg	8	-17021.418	324.182	0	0.925	0.170
Max ~ ISL3 + C1 + C2 + Acc	7	-17020.947	324.653	0	0.925	0.172
Max ~ ISL3 + C1 + C2 + YFU + Acc	8	-17020.167	325.433	0	0.925	0.169
Max ~ ISL1 + C1 + C2 + Acc + pAg	8	-16985.009	360.591	0	0.925	0.171
Max ~ ISL1 + C1 + C2 + Acc	7	-16983.771	361.828	0	0.925	0.173
Max ~ ISL1 + C1 + C2 + YFU + Acc	8	-16982.969	362.631	0	0.925	0.170
Max ~ ISL3 + C1 + C2 + YFU + PD	8	-16956.275	389.325	0	0.925	0.102
Max ~ ISL3 + C1 + C2 + PD	7	-16953.886	391.714	0	0.925	0.099
Max ~ ISL3 + C1 + C2 + pAg	7	-16949.386	396.214	0	0.925	0.087
Max ~ ISL3 + C1 + C2 + YFU	7	-16938.615	406.985	0	0.925	0.075
Max ~ ISL3 + C1 + C2	6	-16934.575	411.025	0	0.925	0.068
Max ~ ISL1 + C1 + C2 + YFU + PD	8	-16919.692	425.908	0	0.924	0.098
Max ~ ISL1 + C1 + C2 + PD	7	-16917.378	428.222	0	0.924	0.095
Max ~ ISL1 + C1 + C2 + pAg	7	-16914.724	430.876	0	0.924	0.083
Max ~ ISL1 + C1 + C2 + YFU	7	-16902.199	443.401	0	0.924	0.070

Model	df	AIC	ΔAIC	ω	R^2_{sp}	R^2_{nsp}
<i>Max ~ ISL1 + C1 + C2</i>	6	-16898.267	447.333	0	0.924	0.062
<i>Skew ~ ISL4 + C1 + C2 + YFU + Acc</i>	8	-39087.951	0	0.519	0.906	0.317
<i>Skew ~ ISL4 + C1 + C2 + Acc + pAg</i>	8	-39087.406	0.545	0.395	0.906	0.314
<i>Skew ~ ISL2 + C1 + C2 + YFU + Acc</i>	8	-39083.217	4.734	0.049	0.906	0.311
<i>Skew ~ ISL2 + C1 + C2 + Acc + pAg</i>	8	-39082.434	5.517	0.033	0.906	0.307
<i>Skew ~ ISL4 + C1 + C2 + Acc</i>	7	-39078.419	9.532	0.004	0.906	0.314
<i>Skew ~ ISL2 + C1 + C2 + Acc</i>	7	-39073.899	14.052	0	0.906	0.308
<i>Skew ~ ISL4 + C1 + C2 + YFU + PD</i>	8	-39064.685	23.266	0	0.906	0.309
<i>Skew ~ ISL2 + C1 + C2 + YFU + PD</i>	8	-39058.958	28.993	0	0.906	0.301
<i>Skew ~ ISL4 + C1 + C2 + pAg</i>	7	-39055.768	32.183	0	0.906	0.303
<i>Skew ~ ISL4 + C1 + C2 + PD</i>	7	-39050.714	37.237	0	0.906	0.304
<i>Skew ~ ISL2 + C1 + C2 + pAg</i>	7	-39049.689	38.262	0	0.906	0.294
<i>Skew ~ ISL4 + C1 + C2 + YFU</i>	7	-39049.130	38.821	0	0.906	0.305
<i>Skew ~ C1 + C2 + YFU + Acc</i>	7	-39049.013	38.938	0	0.905	0.282
<i>Skew ~ C1 + C2 + Acc + pAg</i>	7	-39046.266	41.685	0	0.905	0.279
<i>Skew ~ ISL2 + C1 + C2 + PD</i>	7	-39045.189	42.762	0	0.906	0.296
<i>Skew ~ ISL2 + C1 + C2 + YFU</i>	7	-39043.351	44.600	0	0.906	0.297
<i>Skew ~ C1 + C2 + Acc</i>	6	-39040.131	47.820	0	0.905	0.28
<i>Skew ~ ISL4 + C1 + C2</i>	6	-39031.509	56.442	0	0.906	0.298
<i>Skew ~ ISL2 + C1 + C2</i>	6	-39025.984	61.967	0	0.906	0.29
<i>Skew ~ C1 + C2 + YFU + PD</i>	7	-39024.177	63.774	0	0.906	0.273
<i>Skew ~ C1 + C2 + PD</i>	6	-39010.843	77.108	0	0.906	0.269
<i>Skew ~ C1 + C2 + pAg</i>	6	-39010.802	77.149	0	0.906	0.267
<i>Skew ~ C1 + C2 + YFU</i>	6	-39007.509	80.442	0	0.906	0.270
<i>Skew ~ C1 + C2</i>	5	-38990.505	97.446	0	0.906	0.265
<i>Skew ~ ISL3 + C1 + C2 + YFU + Acc</i>	8	-37855.236	1232.715	0	0.906	0.305
<i>Skew ~ ISL3 + C1 + C2 + Acc + pAg</i>	8	-37854.66	1233.291	0	0.906	0.301
<i>Skew ~ ISL3 + C1 + C2 + Acc</i>	7	-37854.146	1233.805	0	0.906	0.303

Model	df	AIC	ΔAIC	ω	R^2_{sp}	R^2_{nsp}
<i>Skew ~ ISL3 + C1 + C2 + pAg</i>	7	-37852.593	1235.358	0	0.906	0.288
<i>Skew ~ ISL3 + C1 + C2 + YFU</i>	7	-37852.026	1235.925	0	0.906	0.291
<i>Skew ~ ISL3 + C1 + C2 + YFU + PD</i>	8	-37851.322	1236.629	0	0.906	0.295
<i>Skew ~ ISL3 + C1 + C2</i>	6	-37849.351	1238.600	0	0.906	0.284
<i>Skew ~ ISL3 + C1 + C2 + PD</i>	7	-37849.168	1238.783	0	0.906	0.290
<i>Skew ~ ISL1 + C1 + C2 + YFU + Acc</i>	8	-37842.186	1245.765	0	0.906	0.299
<i>Skew ~ ISL1 + C1 + C2 + Acc</i>	7	-37841.148	1246.803	0	0.906	0.297
<i>Skew ~ ISL1 + C1 + C2 + Acc + pAg</i>	8	-37841.019	1246.932	0	0.906	0.296
<i>Skew ~ ISL1 + C1 + C2 + YFU</i>	7	-37839.01	1248.941	0	0.906	0.286
<i>Skew ~ ISL1 + C1 + C2 + pAg</i>	7	-37838.729	1249.222	0	0.906	0.283
<i>Skew ~ ISL1 + C1 + C2 + YFU + PD</i>	8	-37838.575	1249.376	0	0.906	0.290
<i>Skew ~ ISL1 + C1 + C2 + PD</i>	7	-37836.534	1251.417	0	0.906	0.285
<i>Skew ~ ISL1 + C1 + C2</i>	6	-37836.409	1251.542	0	0.906	0.279